



universidade de aveiro
theoria poiesis praxis

UNIVERSITA' DEGLI STUDI DI PADOVA

DIPARTIMENTO DI SCIENZE DEL FARMACO

UNIVERSIDADE DE AVEIRO

DEPARTAMENTO DE QUÍMICA

**CORSO DI LAUREA MAGISTRALE IN CHIMICA E TECNOLOGIA
FARMACEUTICHE**

TESI DI LAUREA

**Synthesis and photophysical evaluation of new porphyrin-azabicyclo conjugates
for PDT and antibiotic therapy**

RELATORE: PROF. GIORGIA MIOLO

CO-RELATORE: PROF. MARIA do AMPARO FERREIRA FAUSTINO

LAUREANDO: Frenzo Federico

ANNO ACCADEMICO 2021-2022

Abstract

La Photodynamic therapy (PDT) è una metodologia fototerapica che funziona attraverso la produzione di specie radicaliche dell'ossigeno (ROS) in seguito a irradiazione, con corretta lunghezza d'onda, di un foto sensibilizzatore in presenza di ossigeno. Questo meccanismo rende la PDT una tecnica utilizzabile in aree come l'identificazione e cura delle forme tumorali, oltre che alla possibilità di debellare malattie causate da agenti patogeni, come virus e batteri. Questa tesi riprende il lavoro di Tessari Francesco, un ex collega proveniente dalla mia università, che trovò un set di molecole potenzialmente utili per la PDT: dei derivati dell'unione tra

5,10,15,20-tetrakis(pentafluorophenyl)porphyrin (TPFPP) e 1,8-diazabicyclo[5.4.0]undec-7-ene (DBU). L'uso di amidine e guanidine azabicycliche, ha come scopo quello di sfruttare il loro comportamento nucleofilo, piuttosto che la loro basicità. DBU ha dimostrato di intraprendere una reazione di sostituzione nucleofila aromatica con TPFPP, portando all'ottenimento di coniugati mono-, di-, tri-, tetra-sostituiti. Tale reazione prevede l'apertura dell'anello del DBU, per formare un derivato dell' ϵ -caprolattame. In questo progetto è stata usata anche 1,5-Diazabicyclo[4.3.0]non-5-ene (DBN), un'altra amidina azabicyclica, per poter avere un altro set di molecole da confrontare con il set di molecole ottenute dalla reazione con il DBU. L'obiettivo di questa tesi è quello di mostrare l'intero processo di caratterizzazione dei due set di molecole: dalla scelta del solvente migliore in cui svolgere la reazione, alle capacità dei due set di molecole di generare radicali liberi dell'ossigeno, per mostrare quali processi siano stati più efficaci rispetto ad altri. Alla fine del Progetto tutti i prodotti saranno stati caratterizzati attraverso UV spectroscopy, fluorescence emission, mass spectrometry, ^1H NMR, ^{12}C NMR, ^{19}F NMR, COSY, HMBC, HSQC, NOESY e singlet oxygen generation test.

Abstract

Photodynamic therapy (PDT) is a form of phototherapy that works by producing reactive oxygen species (ROS) from the irradiation, with a specific lightwavelength, of a photosensitizer in the presence of Oxygen. This mechanism makes PDT applicable in areas such as tumor detection and treatment of cancer and other non-malignant diseases (viruses and bacteria). This thesis continues the work of Tessari Francesco, an older colleague from my university, that found a potentially useful set of molecules for PDT: a 5,10,15,20-tetrakis(pentafluorophenyl)porphyrin (TPFPP) conjugated with 1,8-diazabicyclo[5.4.0]undec-7-ene (DBU). The use of azabicyclic amidines and guanidines, aims at the exploitation of their nucleophilic behavior, rather than their more commonly known basicity. DBU has proved to undergo nucleophilic substitution reaction with TPFPP, leading to the obtainment of mono-, di-, tri- or tetrasubstituted conjugates. The reaction involves the ring opening of DBU, leading to the formation of an ϵ -caprolactam derivative. In this project I also used another base, 1,5-Diazabicyclo[4.3.0]non-5-ene (DBN), another azabicyclic amidines, to produce another set of molecules and compare it to the DBU set.

The aim of this work is to show the whole characterization process of those two compound sets, from the choice of the solvent to the singlet oxygen generation capabilities of all the products, and determinate if they are adequate PDT candidates.

At the end of the project all the products will be fully characterized using UV spectroscopy, fluorescence emission, mass spectrometry, ^1H NMR, ^{12}C NMR, ^{19}F NMR, COSY, HMBC, HSQC, NOESY and singlet oxygen generation test.

ACRONYMS

δ – Chemical shift

Φ_{Δ} – Singlet oxygen quantum yield

Φ_F – Fluorescence quantum yield

λ - Wavelength

λ_{max} – Wavelength of maximum absorbance

μM – Micromolar

aPDT – Antimicrobial Photodynamic Therapy -
doublet

Da – Dalton

DBU- 1,8-Diazabicyclo [5.4.0]undec-7-ene

DDQ – 2,3-Dichloro-4,5-dicyano-1,4-benzoquinone

DMA- Dimethylantracene

DMF - N, N-dimethylformamide

DMSO - Dimethylsulfoxide

DNA – Deoxyribonucleic acid

MS – Mass spectrometry

ESI-MS – Electrospray Ionization Mass Spectrometry

Eq- equivalents

PS – Photosensitizer

GSH – Glutathion in reduce form

GSSG - Gluathion in oxidize form

Hp - Hematoporphyrin

HpD – Hematoporphyrin derivatives

Hz – Hertz

ISC – Intersystem crossing

IUPAC – International Union of Pure and applied Chemistry

J – Coupling constant

LDL – Low density lipoproteinsm

m – Multiplet

M-Multiplicity

$[\text{M}]^+$ - Molecular Ion

MALDI –Matrix-assisted Laser Desorption/ionization

$[\text{M}+\text{H}]^+$ - Protonated molecular ion

MW - Micro-wave

m/z – Mass and charge ratio

NMR-Nuclear magnetic resonance

p-cloranil - 2,3,5,6-tetrachloro-p-benzoquinone

PDI – Photodynamic inactivation of microorganism

PDT – Photodynamic Therapy

Ph - Phenyl

PH₂ – Porphyrin core in the free form

ppm – Parts per million

RT- Room Temperature

s - Singlet

t – Triplet

THF-Tetrahydrofuran

TFA – Trifluoroacetic acid

TLC – Thin layer Chromatography

TPFPP-5,10,15,20-tetraquis(pentafluorophenyl)porphyrin

TPP - 5,10,15,20-tetraphenylporphyrin

UV-Vis – Ultraviolet-visible spectroscopy

Watt

Index

Part I General concepts about porphyrins	9
1.1 introduction.....	9
1.2 Tetrapyrrolic Macrocycles	9
1.2.1 PORPHYRIN DERIVATIVES NOMENCLATURE	10
1.2.3 Chemical and physical properties	11
1.2.4. PORPHYRIN'S REACTIVITY.....	12
1.2.5. SYNTHESIS OF MESO-SUBSTITUTED PORPHYRINS.....	13
1.3 PORPHYRIN APPLICATIONS.....	16
1.4 PDT	
1.4.1 HISTORICAL ASPECTS AND DEVELOPEMENT OF THE PHOTSENSITIZERS	17
1.4.2 PHOTODYNAMIC THERAPY MECHANISM	21
1.4.3 THE TYPE I MECHANISM.....	23
1.4.4 THE TYPE II MECHANISM.....	24
1.4.5 PHOTODYNAMIC THERAPY IN THE CANCER TREATMENT	25
PART II Planning the improvement of a discovered photosensitizer	27
2.1 Aim of this project.....	27
2.1.1 Ideal features of a photosensitizer	27
2.1.2 Fluorine in drugs: reasons for choosing a fluorinated porphyrinoid	27
2.1.3 Nitrogen-containing organic bases: taking advantage of their nucleophilic behavior	28
2.2 Photophysical evaluation: relevant tests	30
2.2.1 UV-Vis characterization	30
2.2.2 Emission properties.....	30
2.2.3 Singlet oxygen generation.....	30
2.3 NMR.....	31
2.4 ICH guidelines	31
2.5 OHMIC.....	32
Chapter III- Experimental section.....	34
3.1 MATERIALS AND EQUIPMENT	34
3.2 METHODS.....	35
3.2.1 TPFPF Synthesis (first method)	35
3.2.3 Solvent Selection.....	36
3.2.4 OHMIC reactions.....	40
3.2.5 General procedure to synthesize TPFPF+DBU compounds	40
3.2.6 General procedure to synthesize TPFPF+DBN compounds	45
3.3 Photophysical results	49
3.3.1 Fluorimetry	49

3.3.2 UV spectrometry analysis.....	51
3.3.3 Singlet Oxygen Generation	53
3.3.4 KI Singlet oxygen generator essay	55
Chapter IV: Conclusions	57
4.1 Main Conclusions.....	57
Chapter V: references	58

Part I General concepts about porphyrins

1.1 introduction

Porphyrins play an important role in biological systems, like the conversion of light to chemical energy (photosynthesis), in electron transfer processes (metabolism) and in the transport of oxygen (respiration).

From the first half of the 20th century, porphyrins have tracked more and more interest in the research field and today they have different applications, such as: solar energy conversion, dangerous substances detection, as biomarkers and for PDT (photodynamic therapy).

This project is going to be focused on the synthesis and characterization of compounds that can be applied in PDT.

1.2 Tetrapyrrolic Macrocycles

Porphyrin derivatives are a class of compounds of natural origin, with 18π -electron aromatic macrocycles, constituted of four pyrrole subunits. The presence of this aromatic conjugated system leads to porphyrin's ability to absorb light in the visible spectrum (3).

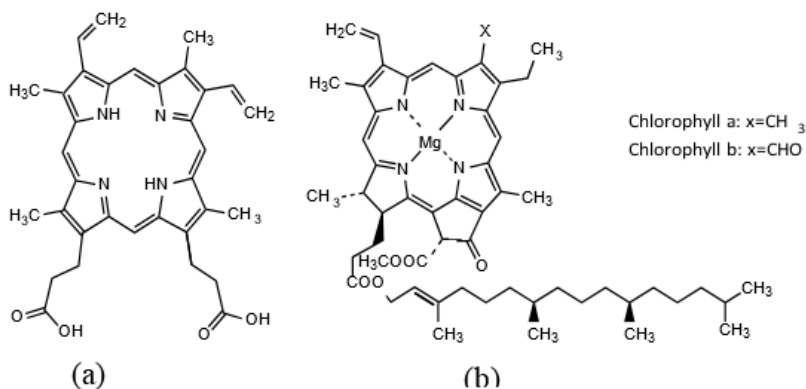
An example of this property can be found in Chlorophyll, characterized by Hans Fischer, a natural complex formed by coordination of magnesium (II) and four inner nitrogen atoms (4). Chlorophyll is the key pigment that guarantees the photosynthesis process (6).

In this process the light is absorbed by chlorophyll molecules and, due to photoexcitation, provides the chemical energy necessary for the conversion of CO_2 and water into carbohydrates -and oxygen (2).

Another porphyrinic group discovered by Hans Fisher, is the heme group structure (Fig.1.1), a complex formed by coordination of iron (II) and four inner nitrogen atoms (4) of protoporphyrin-IX. This group is found in proteins like hemoglobin and myoglobin.

Hemoglobin is present in the red blood cells, ensuring oxygen transport from the lungs to the tissues, as well as the transport of CO_2 from the tissues to the lungs.

Myoglobin is responsible for oxygen storage in muscle cells (4).



The heme group is also present in cytochromes, where it participates in the electron transfer pathways and cellular energy production (5).

1.2.1 PORPHYRIN DERIVATIVES NOMENCLATURE

There are two accepted nomenclature systems for porphyrins. Hans Fischer proposed a simple numbering system where the β -pyrrolic positions are numbered from 1–8 and the α , β , γ , δ positions are called *meso* positions (figure 1.2.1 A). Fischer nomenclature system is not used anymore because it leaves several carbon atoms unassigned in more complicated structures. Nowadays IUPAC has adopted another system which involves the serial numbering of all carbon atoms (figure 1.2.1 B), in which the numeration includes both carbon and nitrogen atoms, considered in sequence (10).

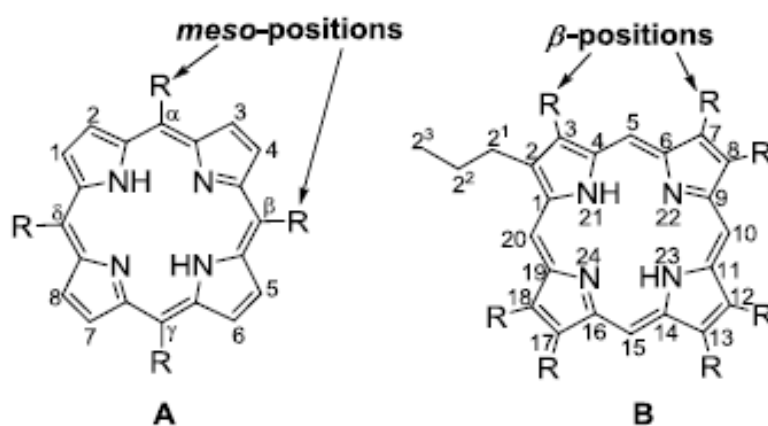


Figure 1.2.1 Fisher nomenclature (A), IUPAC nomenclature (B)

1.2.3 Chemical and physical properties

Porphyrinoids are large aromatic compounds (with diameter of 1-1.5 nm), which present 22 π -electrons in their core (12) (in accordance with Hückel's rule for aromaticity), but only 18 of these participate in the delocalization pathway (4). This highly conjugated π -electrons system is the source of the intense color that porphyrins show (13).

Porphyrin's photophysical properties are unique: they have a wide absorption profile, which goes from the ultraviolet to the near-infrared region of the spectra. This can lead to an electron movement towards the excited state, causing either fluorescence, phosphorescence, or intersystem crossing into an excited triplet state. Their ability to release fluorescence makes them good diagnostic tools, while the reaching of excited triplet state, and subsequent singlet oxygen generation, makes them suitable compounds for photodynamic therapy (3).

Regarding porphyrin's reduction derivatives (figure 1.2.3a), "Chlorins" are porphyrins that have one double bond in β -position, in the porphyrin core, reduced.

"Bacteriochlorin" and "Isobacteriochlorin" are formed when two pyrrolic units are reduced (respectively in opposite and adjacent positions of the core)

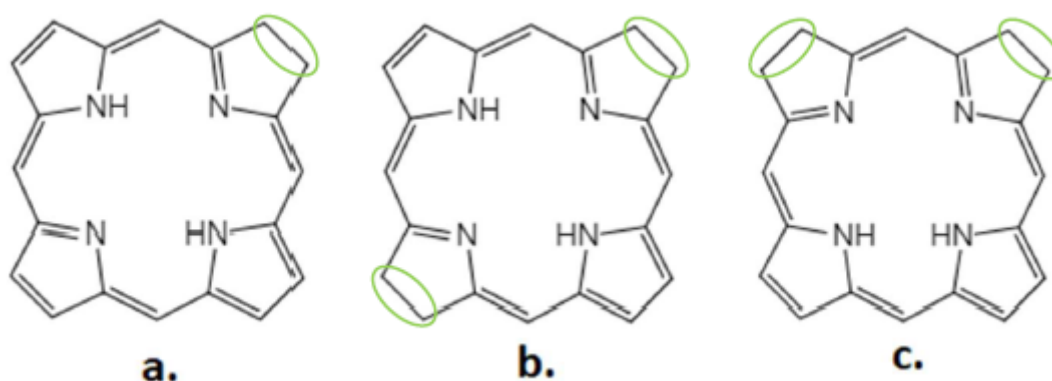


Figure 1.2.3a Chlorin (a), Bacteriochlorin (b), Isobacteriochlorin (c)

The UV-Vis spectra are characterized by the presence of two absorption regions: the first, dominated by the Soret Band, which is characterized by an intense band around 400 nm (11), while Q-Bands are a series of bands of minor, but still relevant, intensity in the area between 500-650 nm (9) (figure 1.2.3b). The Soret Band has almost the same intensity of, magnitude order and localization in every tetrapyrrolic macrocycles (porphyrins, chlorins, bacteriochlorins), as result of the delocalization of the 18 π electrons, so it is not strictly relevant for the characterization (9). On the other hand, the position and intensity of the Q-Bands allows the distinction between porphyrins, chlorins and isobacteriochlorins derivatives. Chlorin presents four Q-bands, one of them around 650 nm with a strong intensity (1,9). Bacteriochlorins show a noticeable band at 750 nm, while isobacteriochlorins have three bands of growing intensity between 500 and 600nm (1, 9).

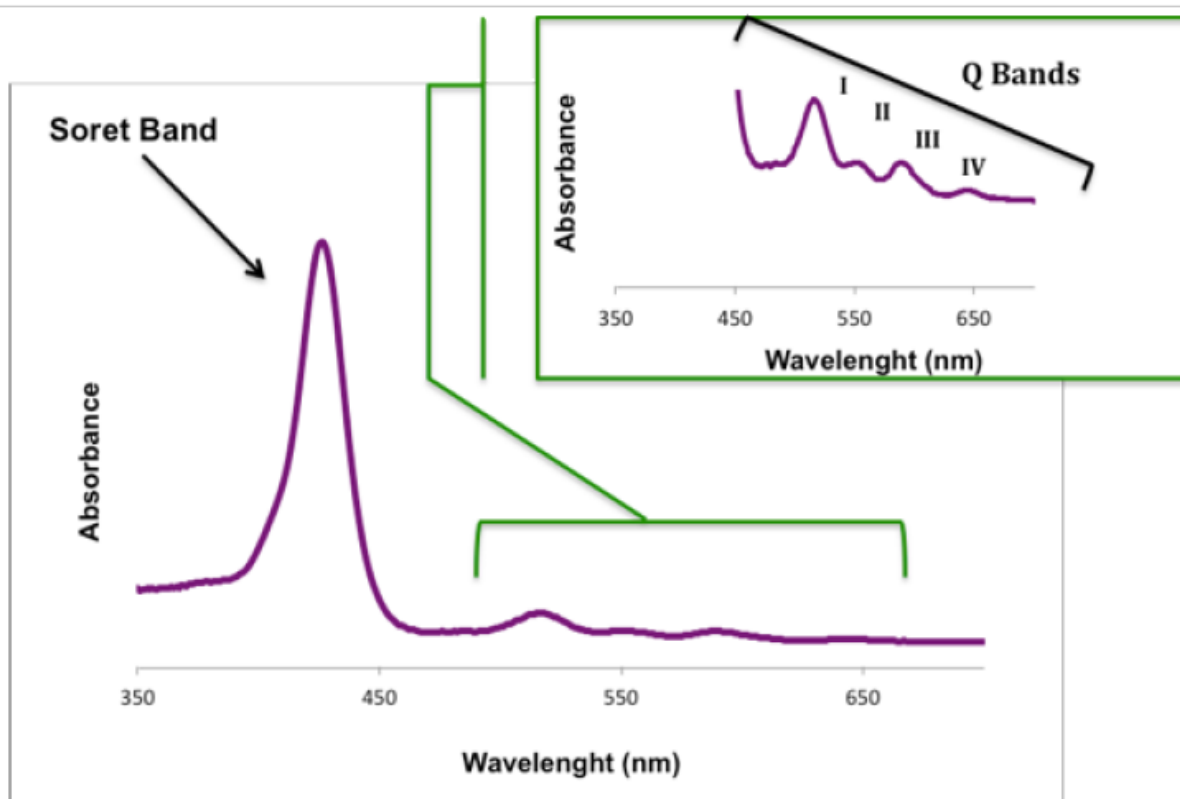


Figure 1.2.3b UV-Vis spectrum of porphyrin derivatives

More changes in the absorption spectra occurs when there is protonation of two of the inner nitrogen atoms, or a metal atom is inserted into the macrocycle. In these situations, there is a more symmetrical geometry than a 7 free base porphyrin, and this leads to the formation of only two Q bands (named α and β) (13),(15).

1.2.4. PORPHYRIN'S REACTIVITY

Porphyrins (PH₂), in their free-base form, may possess basic or acidic properties in solution (Fig. 1.2.4). This property can be attributed to the inner nitrogens.

Two of them are electron donors, and generate the mono and di-cationic derivative in acidic conditions (PH₃⁺ and PH₄²⁺), while the other two, in basic conditions, are electron acceptors and may undergo deprotonation, generating anionic species (PH⁻ and P²⁻) (9,17).

Another feature of porphyrins is the ability to chelate metal ions, in particular bivalent ones such as Mg²⁺, Zn²⁺, Fe²⁺, Co²⁺, Ni²⁺, into their core forming organometallic complexes. In this form, they perform most of their biological activity (8,16). Porphyrin's aromaticity can also be demonstrated by their planar topology and the possibility to participate in electrophilic substitution. Meso-position and the β -pyrrolic positions are subject to this type of reaction (17). Typical electrophilic substitution that may occur in these positions are nitration, formylation, halogenation, acylation, sulfonation and deuteration. The complexation with bivalent metal ions increases the electronegativity of the ring, favoring electrophilic substitution reactions. On the other hand, if the organometallic complex presents a metal with a higher oxidation state like Sn(IV), this leads

to a deactivation of meso-positions and therefore a higher reactivity of β -pyrrolic positions (28). Tetrapyrrolic macrocycles may also undergo aromatic nucleophilic substitution, reduction, or cycloaddition reactions (8).

Studies on porphyrin's reactivity towards different types of conditions allow to predict the best ways to achieve ring's functionalization (23).

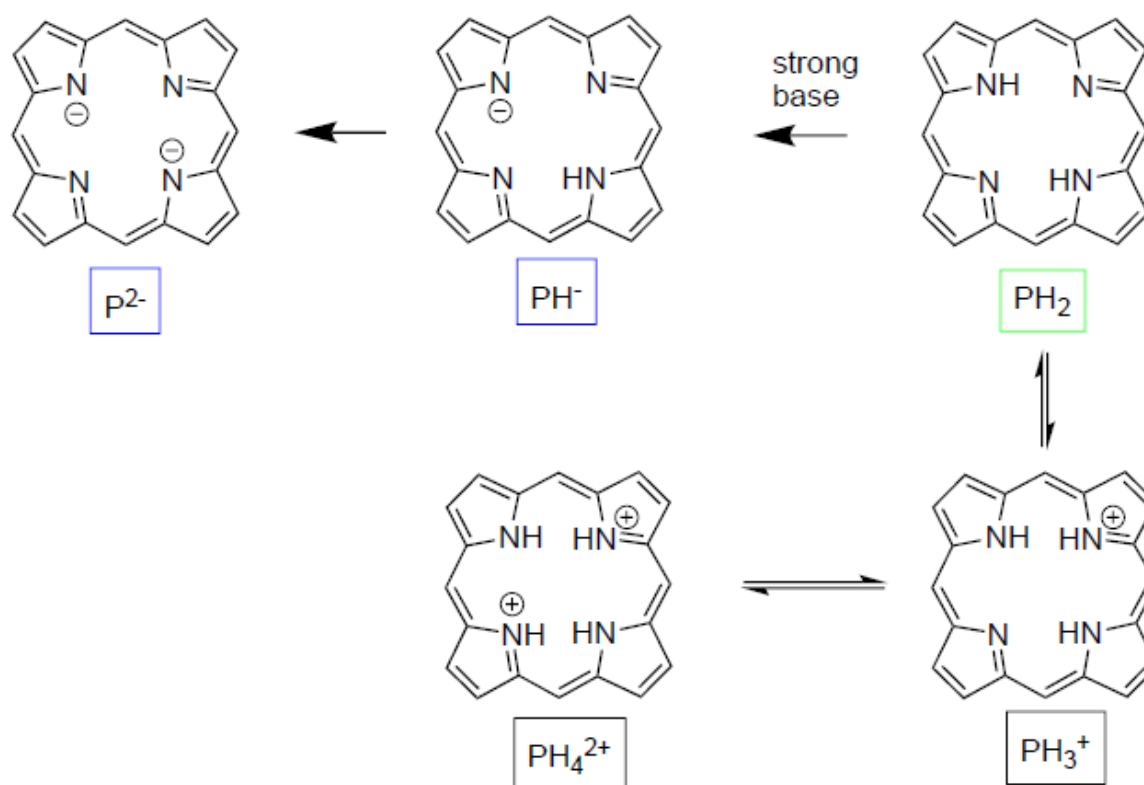


Figure 1.2.4 Acid-base behavior of porphyrin derivatives.

1.2.5. SYNTHESIS OF MESO-SUBSTITUTED PORPHYRINS

As said before, tetrapyrrolic macrocycles may be found in nature, but they can also be synthesized by artificial means. There are several methods to synthesize meso-substituted porphyrin derivatives, which may vary in complexity and number of reaction steps.

The focus of this chapter will be set only on the symmetric meso and tetra substituted porphyrins, as they were the starting material for all the reactions that I performed.

Over the last century many synthesis procedures have been experimented to get these compounds in a good yield. The first approach was performed by Rothmund in 1935

(Figure 1.2.5a) (18, 19), who was able to obtain a 5,10,15,20-tetraphenylporphyrin in 5% of yield, by heating a pyrrole, benzaldehyde, and pyridine solution in a closed vessel at 220° for 48h (18, 20, 21). The yield of that reaction was very low and the product was contaminated by the corresponding chlorin.

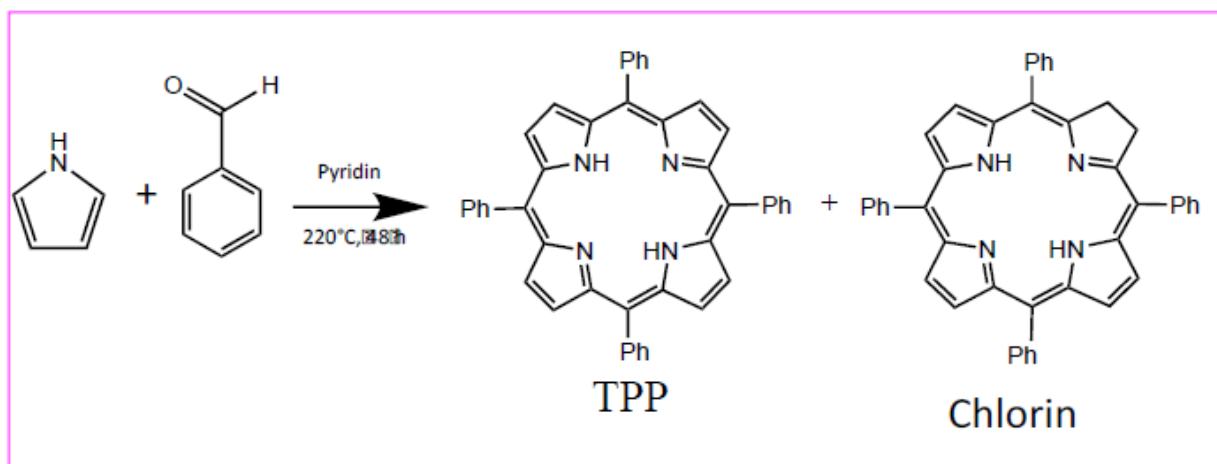


Figure 1.2.5a Rothemund reaction

Later, during the 60's, Adler and Longo (22,26) modified the Rothemund's synthesis method by performing the condensation of benzaldehyde and pyrrole at equimolar ratio, in acidic conditions (propionic acid solution) and in the presence of air. The reaction was carried out in 30 min at reflux and generated TPP with a $20\pm 3\%$ yield in crystalline form (28). This process significantly reduced the formation of the corresponding chlorin (5-10% yield) (22) achieving better results in terms of process performance. The TPP yield, with this method, depends by several factors, such as the acidity of the reaction environment, solvent, temperature, reagents concentration and oxidative atmosphere (22).

Some years later, Lindsey proposed a new route to prepare meso-substituted porphyrins (21,26). The Lindsey methodology it's a two-step synthesis. The first one is the condensation of pyrrole with benzaldehyde in dichloromethane solution, with TFA or BF_3 in catalytic amounts, at room temperature for 30-60 minutes. This step leads to the formation of the porphyrinogen intermediate (figure1.2.5b).

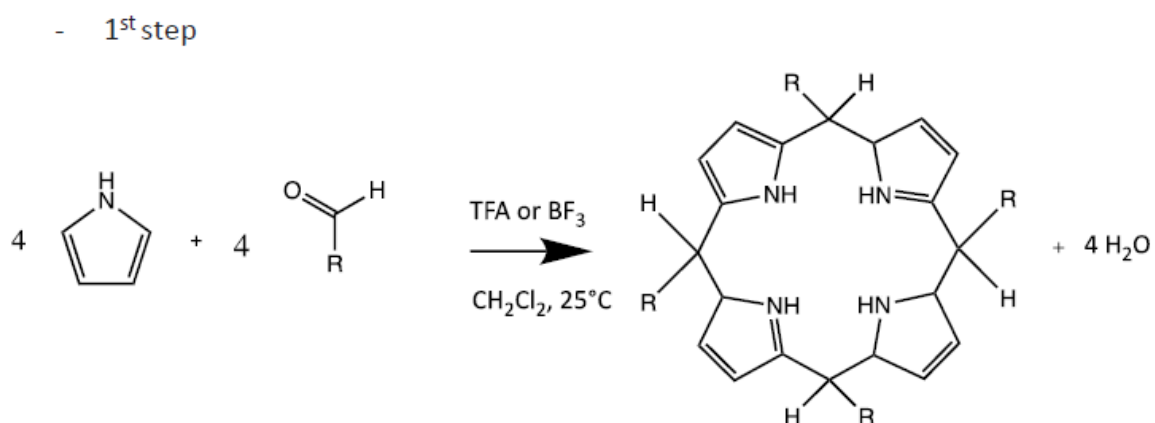


Figure 1.2.5b Lindsey reaction 1st step

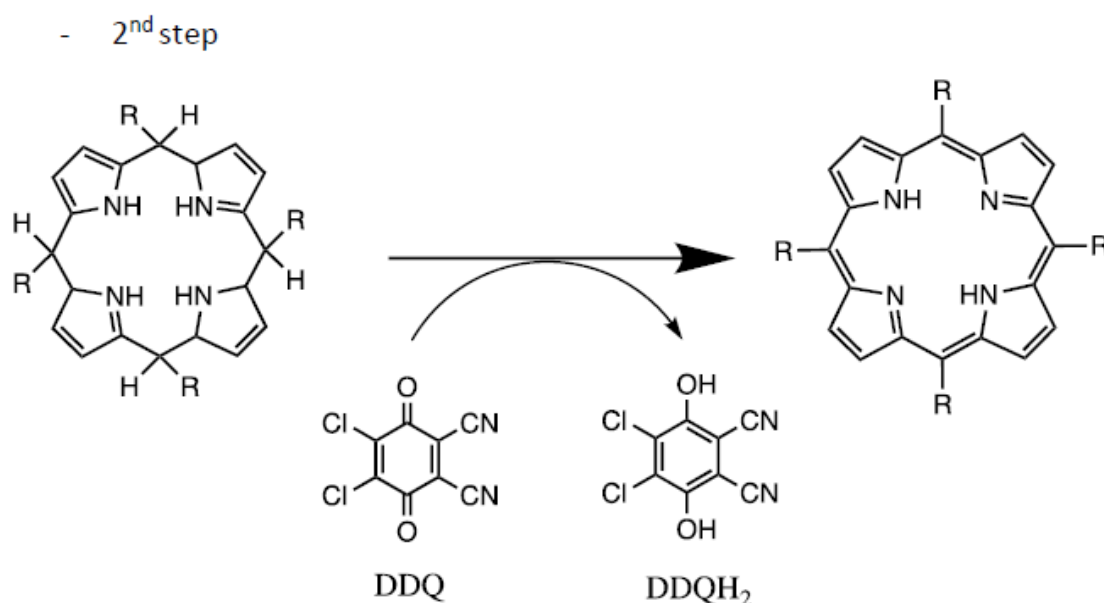


Figure 1.2.5c Lindsey reaction 2ndstep

After that, an oxidant agent, such as DDQ or p-chloranil, is introduced to perform the oxidation of the porphyrinogen into porphyrin. These oxidant agents are also able to convert the chlorin, that has been formed as a side product, into the corresponding porphyrin as shown in the following scheme (Scheme 1.2.5c). Thanks to Lindsey approach the yield of TPP is significantly increased, up to 40% (21). One of the most used and recent methods, was promoted by the scientist Rocha Goncalves and his collaborators (29). He was able to synthesize meso-tetra-arylporphyrins in just one step using acetic or propionic acid as both solvent and catalyst, and nitrobenzene as oxidant agent, performing the reaction for 1hr at 120°C (figure 1.2.5d). Due to the exceptional oxidizing properties of the nitrobenzene, this method avoids the formation of reduced macrocycles, and TPP yield is, more or less, 20% (29). With this simple approach it's possible to get a wide range of symmetric meso-tetra substituted porphyrin derivatives, but it is also an effective way to achieve asymmetrical substituted porphyrins by using a mixture of aldehydes.

Another main advantage of this method is that it avoids the use of high amounts of organic solvents and toxic and expensive quinones.

More recently, Rocha Goncalves and Cavaleiro (28,29) and their research groups improved the process performance using microwave irradiation. The microwave irradiation allows a significant reduction in reaction times and in the quantity of solvents used compared to conventional heating (29) (figure 1.2.5d).

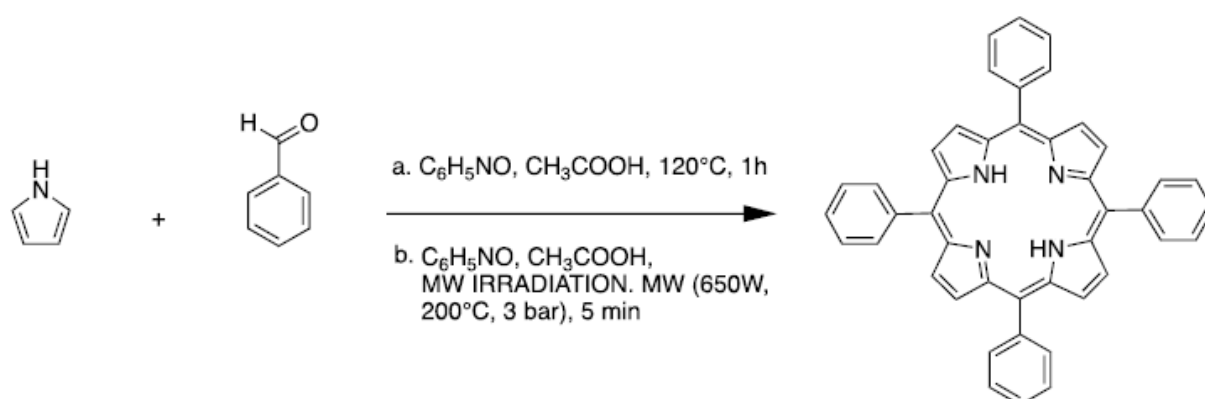


Figure 1.2.5d Synthesis of meso-substituted porphyrins via nitrobenzene. Classic heating (a) and microwaves irradiation (b).

1.3 PORPHYRIN APPLICATIONS

Porphyrin's chemistry studies have grown significantly in recent years, due to their application in different fields, like medicine, catalysis, development of new materials and solar energy conversion.

One important application of metalloporphyrins is as catalysts in the oxidation of a range of organic compounds (40),(41), while fluorinated porphyrinoids can be used as ^{19}F magnetic resonance imaging (MRI) agents (47). The photodynamic reactions carried out by porphyrinoids can be used for antimicrobial purposes (Photodynamic inactivation of bacteria) and for cancer treatment (Photodynamic Therapy, PDT) (39).

Since the aim of this thesis is to synthesize and characterize porphyrinoids that can be used in PDT, its historical and theoretical fundamentals will be analyzed in the next chapters.

1.4 PDT

Photodynamic Therapy (PDT) is a procedure based on the interaction between a photosensitizer molecule (PS), light and oxygen that generates reactive oxygen species (ROS), which leads to cellular damage.

This mechanism is utilized to trigger the destruction of tumor cells and vasculature, and to provide long-lasting protection against metastasis (49)(50).

The application of PDT for cancer treatment is safe and clinically approved, and it has experienced great progresses during the last two decades, making this technique being considered by many scientists as a field with great biological potential for life improvement (7)(50).

1.4.1 HISTORICAL ASPECTS AND DEVELOPEMENT OF THE PHOTSENSITIZERS

Over the centuries, man has always placed great attention on sunlight, seeing its benefits in the medical field and trying to exploit his properties. Phototherapy is the use of visible or near-visible light to treat diseases (30), by involving electronic transitions that lead to photochemical reactions.

Phototherapy can be divided into two broad categories: direct and indirect.

In the direct mechanism the light is absorbed by molecules already present in the organism and no drugs are administered.

In indirect phototherapy an additional substance, called sensitizer, that will absorb the light, is involved (30).

Photodynamic therapy (PDT) can be easily included in the latter category.

The arrival of phototherapy in the modern medicine is due to the Danish scientist Niels Rydberg Finsen (33), who, in the very first years of the 20th century, carried out the research to treat Tuberculosis luposa using light. His discoveries earned him the Nobel Prize for Physiology-Medicine in 1903, and made him unanimously considered the father of modern phototherapy. These concepts were further explored a few years later by the medical student Oscar Raab and the professor Herman Von Tappeiner in Munich.

It was observed that the combined cytotoxic effect of the acrydine, an orange dye, exposed to the light, caused death in the Infusoria, a species of Paramecium, with more efficiency than the two elements alone.

He theorized that the effect was caused by the energy transfer from light to the dye, in a similar way to the photosynthetic process in plants (32).

In the following years Professor Von Tappainer, together with the dermatologist Jesionek (42), administered for the first time a photosensitizer, Eosin, to humans for skin cancer treatment.

The requirement of oxygen in this photosensitization reactions led to the definition of this phenomenon as “photodynamic effect” (32).

In 1913, the physician Mayer-Betz self-injected 200 mg of hematoporphyrin (Hp) causing the body parts that were exposed to the sunlight to suffer pain and swelling for more than 2 months, proving that the phototoxic effects, already seen in mice, could also be induced in humans.

In 1924, Policard (48) theorized the presence and accumulation of endogenous HP in rat's tumor tissue observing fluorescence after exposure to UV radiation (38, 43).

This hypothesis was successfully confirmed by Auler, Benzer (36) and Figge (37) studies. The first two observed fluorescence and necrosis of tumoral tissue after administration of Photodyn (like Hp) after light irradiation, while Figge demonstrated that porphyrins possess a selective affinity for embryonic and regenerating tissues in rats, in addition to the neoplastic one.

In the 60s, Lipson's research group (46) tested the application of a mixture of Hp treated in acidic environment, and discovered that it was more likely to accumulate in rodent neoplastic tissues than pure Hp. Those compounds would be defined as "hematoporphyrin derivative" (HpD) (47, 49).

Following these discoveries, it became a priority to develop a method to get purified fractions of the HpD mixtures, to better understand the biological activity and to improve the performances of this compound class.

Consequently, one decade later, the purified fraction of HpD, called *Stage II* (Fig. 1.8.) in which dimeric and oligomeric structures are present, was utilized as diagnostic agents for cancer. (43)

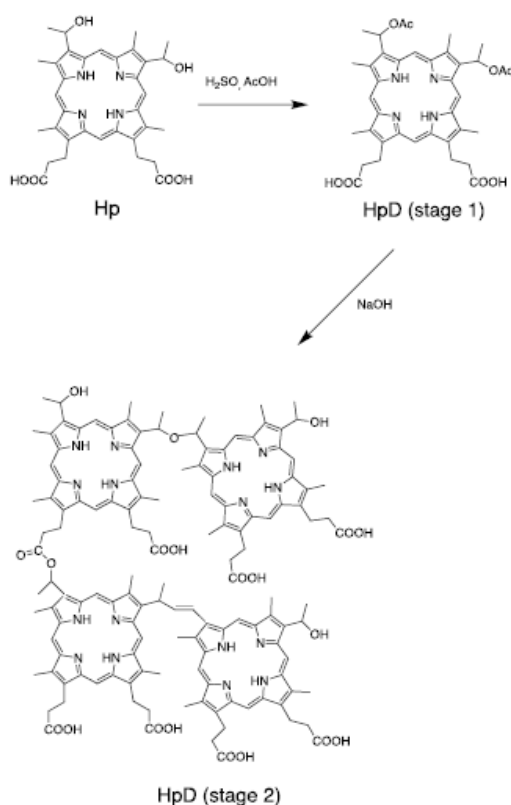


Fig. 1.4.1a Representation of a possible tetrameric form of the HpD mixture (43).

Dougherty work (44) continued in this direction, obtaining a fraction free from heavy oligomeric structures, to which was given the name Photofrin II®.

This fraction was lyophilized by “QLT Phototherapeutics” and “American Cyanamid laboratories” with the denomination Photofrin[®] and now is marketed by the “Pinnacle Biologics, Inc.” (45) and it’s one of the most used photosensitizers worldwide. In 1994 it was used in lung cancer treatment, while in 1995 the FDA approved its use against esophageal cancer. In the same year, Muller and Wilson demonstrated that the administration of Photofrin[®] prolonged the survival in patients affected by malignant glioma (43,53).

Despite the clear benefits that this drug has brought in the treatment of certain types of cancer, it presents some limitations. First, as it’s a mixture of different oligomeric forms, it is difficult to standardize a dose-response relationship. It can also accumulate under the skin for up to six weeks and, if exposed to light, may cause skin photosensitivity.

The last issue with this drug is that the maximum absorption occurs around 630 nm, while maximum light penetration is between 650-800 nm, limiting the operational depth of the compound (38). For these reasons, there has been a need to improve these negative quirks and began the research for new compounds.

The main objective was to obtain pure and standardizable substances, whose overall efficacy was better than first generation PSs (Hp and derivatives). Moreover, these compounds should have absorbed in the red region of the visible spectrum (at $\lambda > 650$ nm) and possessed the ability to target deep neoplastic tissue. In addition, it was very important that these substances were soluble in biological fluids and not toxic when not irradiated (54).

These new derivatives, born from these requirements, were defined as “second” and “third generation”. Second generation of photosensitizers includes benzoporphyrins, phthalocyanines (Pc), Naphthalocyanines (Nc), Chlorines, Porphycenes, Etiopurpurins, *m*-THPC, Texaphyrins (55, 56, 57, 58). Also, among these classes, different molecules have been marketed and used in therapy, like the Foscan[®] (the chlorin *m*-THPC) and Vysudine[®] (also a chlorin derivative) (Figure 1.4.1b).

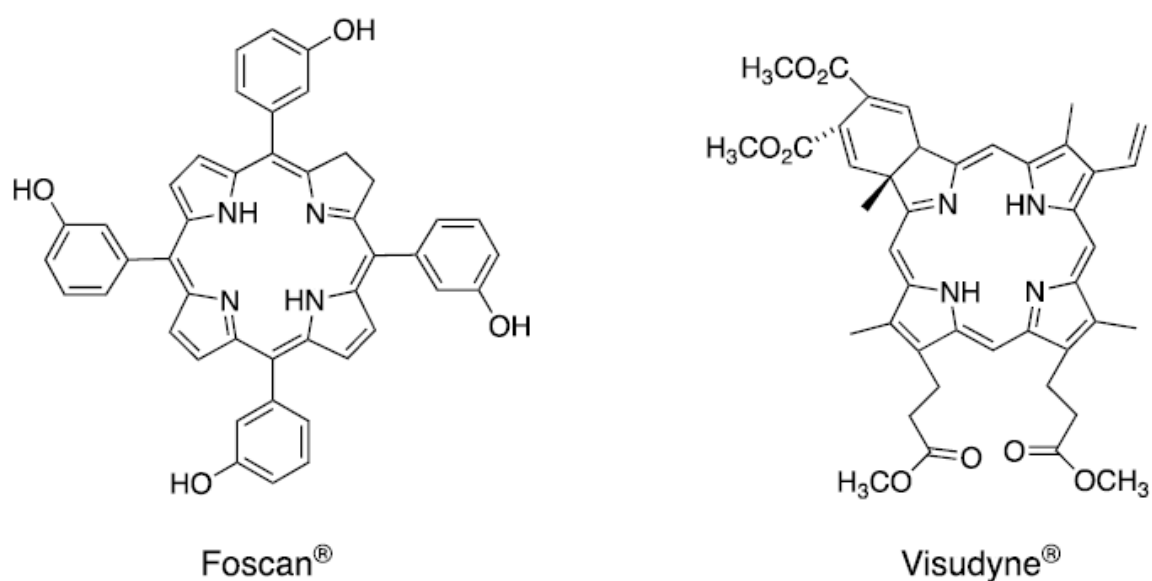


Figure 1.4.1b Structure of Foscan[®] and Visudyne[®]

Every compound of this class is obtained in purified form, therefore it's possible to analyze the dose-response relationship of the drug in a precise manner. In addition, light irradiation at wavelengths above 650 nm can be used in the treatment, resulting in the ability to treat deeper and larger tumors. (52)

The only limitation it's an incomplete selectivity against tumoral tissue (52).

The third generation of photosensitizers is composed of molecules modified to have a better pharmacokinetics, such as being bonded with biomolecules like monoclonal antibodies, protein carriers (56) or nanoparticle systems.

In this way the drug acquires a greater ability to localize itself at the level of tumor tissue, provoking less damage to healthy tissues. (52)

Nowadays PDT is already a widely used technique in clinic, and the development of new compounds seem to have promising results. The main application is still on cancer treatment, particularly in the dermatologic field. Other types of cancer, in which this therapy is being tested on, are lung, esophagus and bladder cancer (57).

In addition to the cancer treatment, PDT can be applied to non-cancer disease too, like psoriasis (58,59), atherosclerosis (61) or age-related macular degeneration (AMD) (60).

In the future it is certain that this technique, thanks to its non-invasiveness, if compared to other therapies, will be more effective and more applicable to old and new pathologies.

1.4.2 PHOTODYNAMIC THERAPY MECHANISM

Photodynamic therapy mechanism has been extensively studied during the last century. The basic principle to induce the photodynamic effect is: by combining the presence of molecular oxygen, light, and a molecule that acts as photosensitizer (a molecule able to absorb and transfer energy from the light source to a substrate) it's possible to form extremely cytotoxic derivatives, like singlet oxygen (1O_2), hydrogen peroxide (H_2O_2), or free radicals such as superoxide anion radical (O^-) and hydroxyl radical $[OH\cdot]$ causing tissue damage. (62,63,64)

The photophysical process involved in PDT is shown in the following *Modified Jablonski Diagram* (Figure 1.4.2a). The diagram illustrates what happens at the photosensitizer's binding electron's level after the absorption of an appropriate electromagnetic wavelength. The fundamental (or ground) electronic state is defined as S_0 , representing the lowest energy level. When the electrons absorb the energy source, their energy level rises to the first excited singlet-state S_1 . This excited state is unstable, and it quickly returns at its fundamental energy state S_0 ($10^{-9} - 10^{-6}$ s). This energetic regression, or relaxation, manifests itself mainly in two ways:

- Radiative decay processes (emission of electromagnetic radiations), such as fluorescence and phosphorescence.
- Not radiative decay processes (heat), as vibrational relaxation, internal conversion, and intersystem crossing.

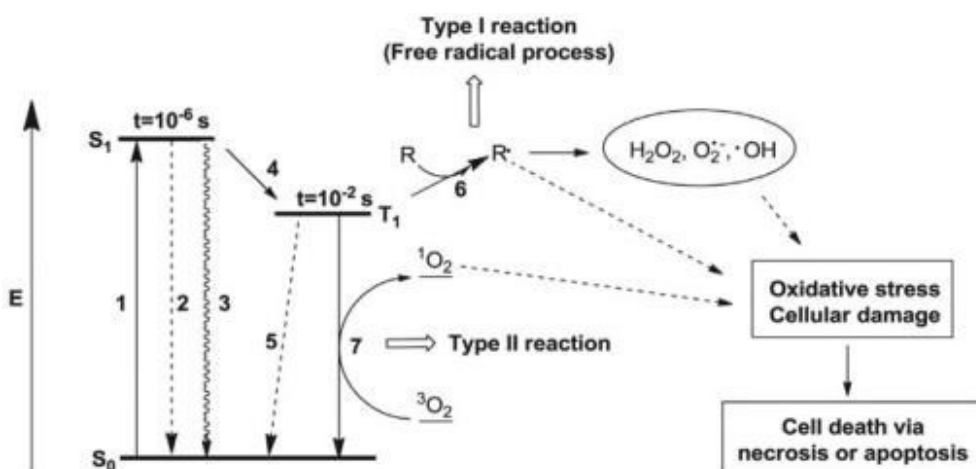


Figure 1.4.2a Modified Jablonski diagram. Processes: 1. absorption; 2. fluorescence; 3. internal conversion; 4. intersystem crossing; 5. phosphorescence; 6. Formation of radical species (type I mechanism); 7. formation of singlet oxygen (type II mechanism) (63).

If there is light emission, it's important to underline that the emitted light is less energetic than the absorbed one and will have higher wavelength.

The transition from the fundamental state S_0 to the Singlet state S_1 is *spin- permitted*, because the antiparallel spin orientation is maintained as well as the multiplicity (Fig 1.4.2b).

$$\begin{aligned} S &= \text{quantum spin number} \\ S &= \sum s_i = +\frac{1}{2}, -\frac{1}{2} \text{ (antiparallel spin)} = 0 \\ M &= 2s+1 = 1 \end{aligned}$$

However, it may occur that the PS converts to the first excited triplet state (T_1) by intersystem crossing (ISC). This state is characterized by a lower level of energy than S_1 , and it's a consequence electronic spin orientation change, from antiparallel to parallel (Fig 1.4.2b.).

$$\begin{aligned} S &= +\frac{1}{2}, +\frac{1}{2} \text{ (parallel spin)} = 1 \\ M &= 2s+1 = 3 \text{ (triplet state)} \\ \text{Transition: } &ISC \end{aligned}$$

This transition is *spin-forbidden*, making it slower (43). This state is named triplet because of the multiplicity.

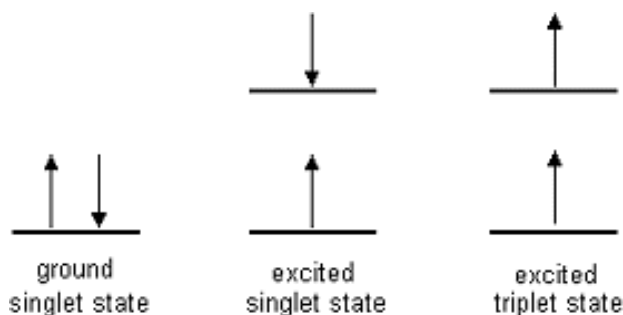


Figure 1.4.2b Electron Spin orientation in singlet ground state, singlet excited state and triplet excited state.

Similarly, to what happened for the singlet state, the electrons tend to return to its fundamental energy state S_0 , but slower than the excited state S_1 to S_0 (10^{-3} - 10 seconds).

The transition from T_1 to S_0 , as for S_1 to S_0 , manifest itself through the release of energy in the form of light emission. This phenomenon is called phosphorescence.

Phosphorescence is characterized by longer wavelengths than fluorescence. That's because the energy difference between T_1 and S_0 is lower than in S_1 and S_0 .

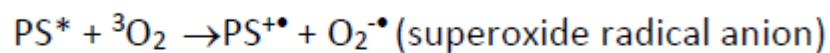
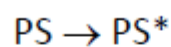
In addition, it's a slower process, and it's less likely to occur since it's a forbidden transition. Despite this, a good PS has a high triplet-state yield, allowing it to interact with other molecules, like Oxygen (65,66).

Once in the triplet state, the PS can react according to two different types of photooxidative reactions, known as type I and type II mechanisms.

1.4.3 THE TYPE I MECHANISM

In type I mechanism (figure 1.4.3), the excited PS can either take an electron from O_2 (a.), with the formation of a superoxide by photooxidation, or electron/proton transfer from an organic substrate (b.), originating a radical cation and superoxide anion, by photoreduction (73).

a.



b.

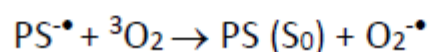
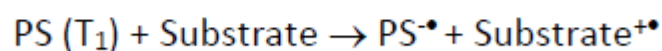


figure1.4.3 Type I mechanism: electron transfer from the excited PS to 3O_2 (a.) and to a molecular substrate (b.), leading to the formation of superoxide radical anion ($O_2^{-\bullet}$).

The superoxide anion by itself is not capable of major oxidative tissue damage, but it can undergo dismutation by superoxide dismutase (SOD), generating hydrogen peroxide (H_2O_2). The $O_2^{-\bullet}$ can also reduce metal ions, like ferric ion (Fe^{3+}) to its ferrous form (Fe^{2+}), catalyzing the conversion of H_2O_2 in hydroxide ion (OH^-) and hydroxyl radical (OH^\bullet), an extremely reactive product, that starts a chain of oxidative reactions (Fenton Reaction) responsible for tissue damage. In addition, superoxide anion can react with the hydroxyl radical to produce singlet oxygen, or with nitric oxide to form another highly reactive species: peroxy nitrite ($OONO^-$) (74).

Singlet oxygen and superoxide anions can react directly and cause damage to biomolecules such as proteins, lipids, steroids, and nucleic acids, causing cytotoxicity (51).

1.4.4 THE TYPE II MECHANISM

With this mechanism, the PS excited triple state directly transfers energy to ground state oxygen, to form singlet oxygen.

This kind of reaction has a simpler mechanism and is generally thermodynamically favored for red-absorbing PSs, occurring preferentially than the type I reaction.

The singlet oxygen reacts with membrane lipids, resulting in lipid peroxidation and increased membrane permeability or membrane disruption.

It also reacts with amino acids, compromising proteins functionality.

Protein amino acid residues tryptophan, tyrosine, histidine, cysteine, and methionine are some of the major targets of ROS. DNA nucleotides are also susceptible to this kind of oxidation, causing DNA strand rupture or DNA-protein cross-link leading to cell death (74)(51).

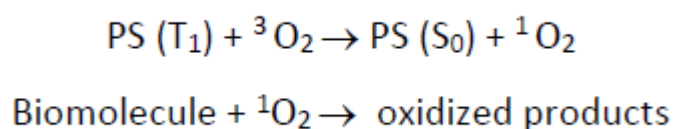


figure1.4.4 Type II mechanism: formation of singlet oxygen and biomolecule's oxidation.

A schematic comparison between the two pathways is shown in figure 1.4.4.

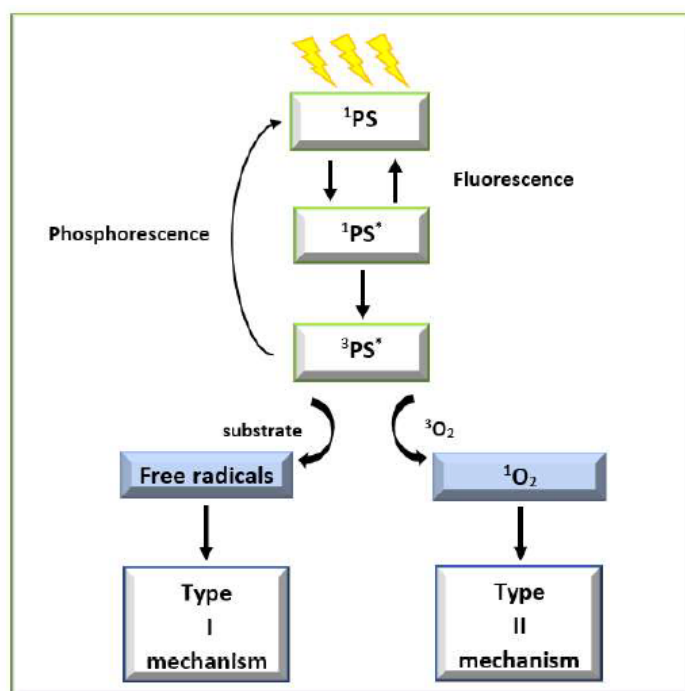


Figure 1.4.4 comparison between type I and Type II mechanism

1.4.5 PHOTODYNAMIC THERAPY IN THE CANCER TREATMENT

Radiotherapy and Chemotherapy, commonly used for cancer treatment, can induce dangerous side effects due to their indiscriminate destruction of both healthy and ill tissues, causing serious physical and psychological degradation.

Consequently, the objective for new cancer treatment therapies is to reduce or eliminate the common side effects of traditional therapies, while maintaining high efficacy. Photodynamic therapy (PDT) is a quite new technique for the treatment of various types of malignant tumors, developed to meet these requirements. Porphyrins and derivatives are the most studied and used in this field, and some of them accumulate selectively in tumor tissues (31).

PDT also, found great success when applied to non-malignant diseases, such as psoriasis or age-related macular degeneration (31,43).

The most common PS administration way is the intravenous one, which generally leads to the PS's binding to low-density lipoprotein (LDL) in the blood stream.

LDLs tends to accumulate in the tumoral tissue, due to increased demand for cholesterol, and this fact, combined with less lymphatic drainage (38), facilitate the accumulation and retention of bound PSs (68). Another important parameter is the pH, as most porphyrin derivatives are not very soluble at physiological pH, while they are much more soluble at lower pH.

Tumor tissue pH is generally lower than in healthy tissues, due to the uncontrolled catabolism in cancer cells, contributing to PSs accumulation (67,69).

The efficiency of a PS is not dictated only by its ability to accumulate itself at cancer cells level, even if this is a fundamental aspect, but also by its ability to generate, by irradiation with the correct wavelength, singular oxygen (1O_2) or other reactive oxygen species (ROS) capable of cellular damage.

The choice of the best wavelength to excite the PS depends, not only on the absorption properties of the molecule, but also on the type of treatment being performed.

In the treatment of non-superficial tumors, the use of low wavelengths, like those of the Soret Band (blue region, around 420 nm), is not appropriate because at a lower wavelength corresponds a lower penetration in the tissues (43) (fig 1.4.5).

Light radiation in the red region is sufficient for an effective penetration, due to less dispersion.

The area of maximum light penetration, named the "Phototherapeutic Window", is between 650 and 800 nm.

Since singlet oxygen is very reactive, its lifetime in water is in the order of 40 ns and with a maximum action radius of 20 nm. Those two aspects, together with localized PS activation by irradiation, allows PDT to be very specific and controllable.

As a result of the irreversible oxidative destruction of key biomolecules and cell structures, three main tumor cell death mechanisms can follow PS's administration: necrosis, apoptosis, and autophagy. The extension of each cell death mechanism depends on the cellular organelles damaged, determined by the intracellular localization of the PS at the time of irradiation (51)(75).

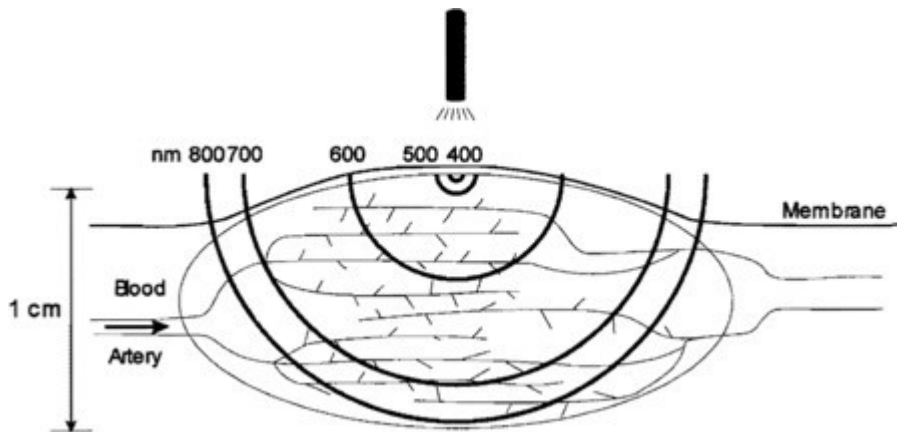


figure 1.4.5 light penetration in the tumor tissue at different wavelengths (43).

Another important factor that affects the outcome of PDT is how the PS interacts with the cellular structures within the tumor.

The most important structural features that affect PS cellular accumulation are the net ionic charge, the degree of hydrophobicity (logarithm of the octanol/ water partition coefficient) and the degree of asymmetry of the molecule (70).

It can be said that the more a molecule is hydrophobic, the more it will tend to cross cellular membranes, and relocate into cellular organelles, mainly at the level of their membranes (70).

The PS can localize within many different cell organelles such as plasma membranes, endoplasmic reticulum, mitochondria, lysosomes, and Golgi apparatus (70).

An apolar PS, when activated, generates singlet oxygen (1O_2) and other ROS, leading to the disorganization of the membranes, cholesterol peroxidation and unsaturated phospholipids.

Polar PSs are not able to pass through the plasma membrane and must undergo endocytosis process to get inside tumor cells. It has been demonstrated that these PSs localize in lysosomes, causing their destruction when activated, leading to leakage of the lysosomal content into the cytoplasm (42). It has also been demonstrated that most PSs are not able to reach and accumulate inside cell's nucleus that have not been exposed to mutation or DNA damage (71).

It is also possible to use the fluorescence emission that most PS can generate at high yields, to localize with precision its location, and therefore the tumor location (71,72).

PART II Planning the improvement of a discovered photosensitizer

2.1 Aim of this project

Following the results of Tessari Francesco work, the aim of this project is to plan the experimental conditions to carry out the nucleophilic substitution of TPFPP with the organic bases DBU and DBN, and the products full characterization.

The expected products are various substitution degrees porphyrinoids which have never been studied before.

The new photosensitizers will then receive a proper photophysical and spectroscopical evaluation to determine which compounds could be suitable candidates for PDT.

It is therefore planned the submission of the final products to specific studies, such as UV-Vis characterization, HNMR, CNMR, FNMR, emission properties analysis and ROS-generation.

OHMIC, as heating method, will be tried too, to see if it's possible to perform the reaction in H₂O or aqueous solvent.

2.1.1 Ideal features of a photosensitizer

Any potential PS should fulfil certain requirements.

Its chemical and physical properties should permit to synthesize a pure compound with good yield in few steps. It should be stable with adequate shelf-life and with polar or amphiphilic features to permit easy and painless administration, without allergic reactions or hypersensitivity (non-water-soluble PSs require a delivery vehicle and have shown to have longer clearance times).

Its absorption band should be high, preferably in the near infrared for optimal tissue penetration, with enough energy to generate singlet oxygen and appreciable fluorescence quantum yield. The longer the light wavelength is, the deeper it will penetrate the tissue (76).

Finally, it should be commercially feasible to produce, with inexpensive materials needed for its production.

2.1.2 Fluorine in drugs: reasons for choosing a fluorinated porphyrinoid

The replacement of a hydrogen by a fluorine can significantly influence pharmacological outcomes, metabolic stability, selectivity, and physical properties (77).

Fluorine is the smallest element in the group of halogens and the most electronegative atom.

It can form high strength bonds providing resistance to temperature and oxidants (78). It can significantly alter the biological properties of a molecule, modulating the lipophilicity, basicity, bioavailability (introducing a fluorine atom next to a basic group can reduce its basicity, enhancing its membrane permeability) and electronegativity.

Although the substitution of hydrogen with fluorine does not have a profound steric influence, electrostatic interactions with other groups can change the molecule's conformation significantly. Fluorine substitution on aromatic rings is also known to increase binding affinity, increasing electrostatic interactions.

Structurally, fluorinated drugs present the fluorine atom in phenyl rings, heterocyclic rings, steroids, and derivatives (78).

Fluorine atom insertion in pyrrolic macrocycle's structures may enrich them with the required pharmacokinetic features to be suitable photosensitizers or diagnostic agents (78).

Regarding the development of new generation of PDT agents, meso-substituted tetrapyrrolic macrocycles are used as the main starting porphyrinoids.

5,10,15,20-tetrakis(pentafluorophenyl) porphyrin (TPFPP) is an interesting template to be functionalized through nucleophilic substitution reactions (figure 2.1.2) (77).

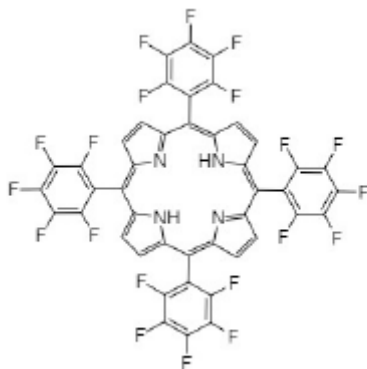


Figure 2.1.2 5,10,15,20 tetrakis(pentafluorophenyl) porphyrin (TPFPP)

2.1.3 Nitrogen-containing organic bases: taking advantage of their nucleophilic behavior

TPFPP's structure is a good scaffold to start with, as it can undergo nucleophilic aromatic substitution reactions.

Strong bases, able to generate the reactive alkoxide, such as Nitrogen-containing organic bases that has an imino group attached to the α - carbon of the amine, are good candidates for this kind of reaction (80).

Some of the most utilized compounds are 1,8-diazabicyclo [5.4.0] undec-7-ene (DBU), 1,5-diazabicyclo[4.3.0]non-5-ene (DBN), methyl-1,5,7-triazabicyclo[4.4.0]dec-5-ene (MTBD) and 1,5,7-triazabicyclo[4.4.0]dec-5-ene (TBD).

The high basicity of these reagents is given by the sum of several intrinsic properties such as: their sp^2 - hybridization on the deprotonated nitrogen atom, their conjugate acid resonance stabilization, and a bicyclic ring system enforces overlap of lone pair electrons of the sp^3 -hybridized nitrogen(s) into the neighboring π^* orbital, increasing electron density on the sp^2 -hybridized nitrogen (81).

Among these bases, DBU has been widely studied and used as a catalyst and a reagent in dehydrohalogenation reactions (82)(83). Its application as a base to synthesize porphyrin-flavone conjugates leads to monosubstituted conjugates, but also a by-product of a porphyrin-DBU conjugate (84). This is due to DBU's nucleophilic behavior, that brings it to compete with the alkoxide for the reaction with TPFPP. The nucleophilic reaction is followed by a ring-opening in the base's structure, leading to the product shown in figure 2.1.3a.

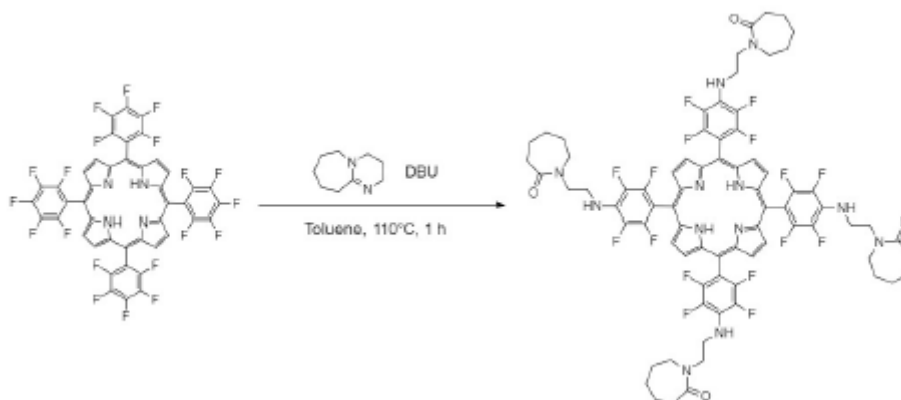


Figure 2.1.3a Synthesis of the TPFPP-DBU conjugate.

This kind of reactions are expected to occur following two potential pathways (figure 2.1.3b). The first (a.) involves the initial hydrolysis of the amidine to generate a primary amine, which can then react with an electrophilic group, is expected when water is present in significant amount. The other path (b.) describes amidine's interaction with the electrophile to produce a cationic intermediate that can react with water molecules, occurring in anhydrous conditions (81). Nitrogenous bases are not stable in aqueous mixtures, and they will hydrolyze to some degree if the reaction is run in the presence of water, in aqueous workups and for crystallizations, even under mild conditions, generating aminolactams and aminoureas. (81). The nucleophilic behavior of DBU and the ring-opening properties, will be used to synthesize different levels of conjugation of TPFPP and DBU. The conjugation with DBN will also be investigated

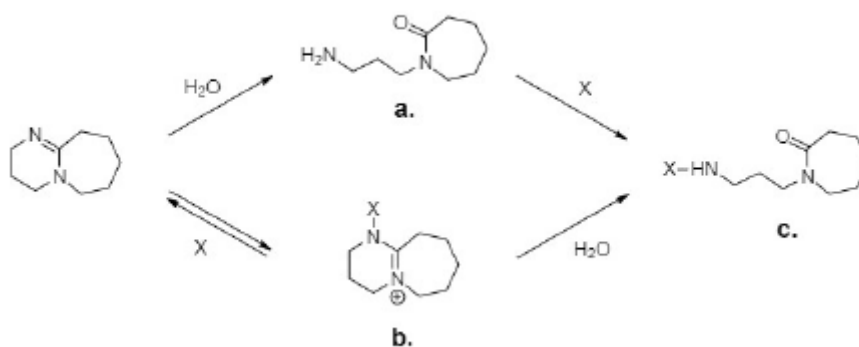


Figure 2.1.3b Two potential pathways for the bases to react with the electrophilic group (X) [101].

2.2 Photophysical evaluation: relevant tests

The photophysical evaluation of the final products is done to confirm the identity of the synthesized conjugates and if they are suitable PDT photosensitizers.

2.2.1 UV-Vis characterization

The UV-Vis absorption spectrum it's an easy and quick way to check the nature of the compound and to determine what is the maximum absorption wavelength for each molecule. For porphyrin rings, the presence of the Soret band around 400 nm is predictable, as well as the Q bands at longer wavelengths. Given the absorbance at the maximum absorption wavelength, it is possible to calculate the molar absorption coefficient (ϵ) of the Soret band and of the Q bands. Knowing the absorption region of each PS is required to establish which light source will be useful to activate against tumor cells.

2.2.2 Emission properties

Fluorescence is a phenomenon through which a photosensitizer emits the previously absorbed electromagnetic radiation, with a higher wavelength, returning to the ground energy state from its excited state. It is important to study the emission spectrum of a PS to analyze the quantity of energy dissipated, rather than transferred to other substrates.

Fluorescence properties are a useful characteristic in the diagnostic field, and the use of PSs as markers for tumor detection is constantly evaluated.

2.2.3 Singlet oxygen generation

To be considered as a photosensitizer candidate in PDT, the obtained conjugates must be able to generate ROS upon exposure to light, causing cell death.

One of the main ROSs responsible for the photodynamic effect is $^1\text{O}_2$, the ability of the conjugates to generate $^1\text{O}_2$ can be assessed using an indirect method that monitors the decomposition of Dimethylacetamide (DMA) in the presence of the PS upon irradiation with a red light at 630 ± 20 nm in DMF.

The combination of light, porphyrin derivative and oxygen will produce $^1\text{O}_2$, which reacts with DMA, inducing a decay of the DMA absorption band (87).

The production of iodine (I_2) can be another method to assess if a PS could be a suitable candidate for PDT. This effect results from a series of reactions between KI and singlet oxygen, which originates peroxyiodide that can decompose into free iodine or reactive iodine radicals both with oxidative properties. Having this in mind, the production of iodine (I_2) by a PS in the presence of KI can be assessed by irradiating, with white light (380–700 nm; LED system–25 mW.cm⁻²) (87) and measuring the absorbance at 340nm afterwards. The more I_2 will be produced, the higher the absorbance.

2.3 NMR

The nuclear magnetic resonance (NMR) is another useful technique for porphyrin characterization (1). ¹HNMR provides clear spectra in which the signal generated by the resonance of the NH protons appears around -2/-4 ppm because of the strong electronic shield due to the ring current displayed around the macrocycle. The same ring current is responsible for the unprotection of β-pyrrolic and meso-protons that are consequently shifted to lower fields and appear at chemical shift between 8 and 11 ppm (12,14,15).

¹⁹FNMR was also used to distinguish the different degree of substitution between the compounds generated by the conjugation of TPFPP and DBU/DBN.

2.4 ICH guidelines

ICH guidelines are a set of guidance's made to ensure that safe, effective, and high-quality medicines are developed and registered efficiently.

The objective of this guideline is to recommend acceptable amounts of residual solvents in pharmaceuticals, to ensure the safety of the patient.

Even if the compounds that will be synthesized in this research won't be used in practice, it's better to develop a synthesis route that employs solvents that could potentially be used according to the ICH guidelines.

Residual solvents in pharmaceuticals are defined as organic volatile chemicals that are used or produced in the manufacture of drug, substances or excipients, or in the preparation of drug products (85). The solvents are not completely removed by practical manufacturing techniques. Appropriate selection of the solvent for the synthesis of drug substance may enhance the yield, or determine characteristics such as crystal form, purity, and solubility. Therefore, the solvent may sometimes be a critical parameter in the synthetic process. (85)

Since there is no therapeutic benefit from residual solvents, all of it should be removed to the extent possible to meet product specifications, good manufacturing practices, or other quality-based requirements. Drug products should contain no higher levels of residual solvents than what is reported by safety data. Some solvents that are known to cause unacceptable toxicities (Class 1) should be avoided in the production of drug substances, excipients, or drug products unless their use can be strongly justified in a risk-benefit assessment. Some solvents associated with less severe toxicity (Class 2) should be limited to protect patients from potential adverse effects. Ideally, less toxic solvents (Class 3) should be used where practical. (85)

Solvents were evaluated for their possible risk to human health and placed into one of three classes as follows:

Class 1 solvents: Solvents to be avoided

Known human carcinogens, strongly suspected human carcinogens, and environmental hazards. They should not be employed in the manufacture of drug substances, excipients, and drug products because of their unacceptable toxicity or their deleterious environmental effect (85)

Class 2 solvents: Solvents to be limited

Non-genotoxic animal carcinogens or possible causative agents of other irreversible toxicity such as neurotoxicity or teratogenicity. Solvents suspected of other significant but reversible toxicities. (85)

Class 3 solvents: Solvents with low toxic potential

Solvents with low toxic potential to man; no health-based exposure limit is needed. Class 3 solvents have PDEs of 50 mg or more per day. (85)

2.5 OHMIC

Ohmic heating was used in this project to test if it's possible to do the conjugation reaction in water, or in other aqueous solutions. It was just a test and I included it for the sake of completion.

Ohmic heating is defined as a process in which the material to be heated (for example a reaction mixture), is heated by passing an AC electrical current through it. Ohmic heating differs from other heating methods because it involves the use of electrodes that are in direct contact with the medium to be heated. (86)

The frequency applied is variable in opposition to microwave heating (use of radiation with a frequency of 2.45 GHz) and lower than the microwave and radio frequencies. The waveform (sinusoidal, triangle or square) is not restricted, but the sinusoidal waveform is more frequently used (Figure 2.4a).

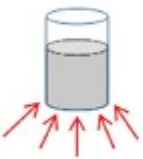

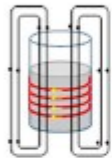
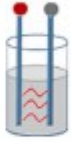
Heating method			
Conventional, CH	Microwave irradiation, MW	Inductive, IH	Ohmic, CH
			
The energy is transferred through the walls of the reaction vessel and then dissipated into the reaction mixture.	Direct and internal absorption of microwave radiation by the molecules present in the reaction mixture.	Joule effect resulting from induced electric current in the medium. Continuous or alternating field.	Joule effect resulting from the passage of alternating electric current. Electrodes in contact with the medium.

Figure 2.4a Main heating methods used in organic synthesis.

In microwave, and ohmic heating the heat is generated internally, by the electrical energy transformation into heat due to ion movement and friction. However, ohmic heating allows a more uniform and deeper heating, than microwave because the extent of heating is governed only by the spatial uniformity of electrical conductivity throughout the reaction medium and the reaction time or residence time (in flow conditions).(86)

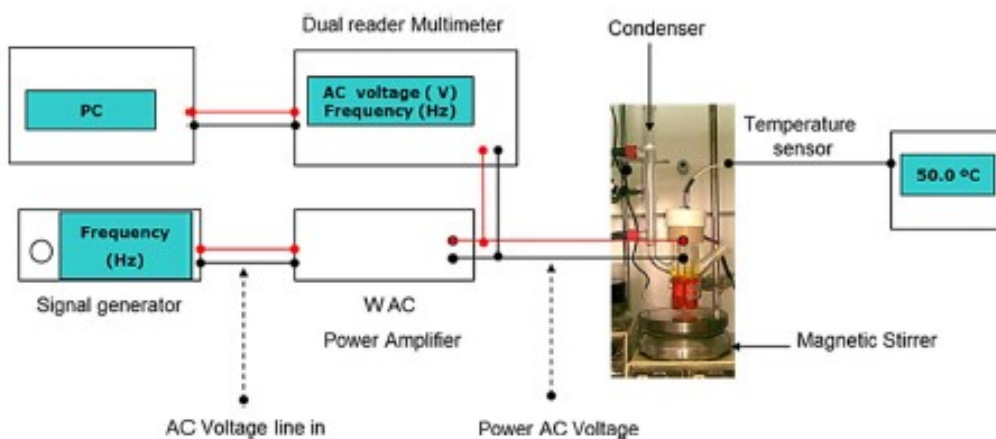


Figure 2.4b Schematic representation of the ohmic heating reactor (Portuguese Patent No. 105908, 2011-09-27).

Chapter III- Experimental section

3.1 MATERIALS AND EQUIPMENT

- commercial reagents
- PA grade solvents for crystallization.
- Thin layer chromatography (TLC), using plastic sheets coated with silica gel 60, to check reactions.
- Merck gel silica 60 of 0.063-0.200 mm, for column separation.
- Preparative TLC, using glass plates (20 x 20 cm), coated with a layer of silica gel 60 (Merck) 0.5 mm and suddenly dried for 10 h at 100°C in the oven.
- ¹H, ¹²C, ¹⁹F NMR spectra and COSY, HMBC, HSQC, NOESY spectra were recorded on a Bruker AMX 300 apparatus. The solvents used was deuterated chloroform.
- Mass spectra were recorded in a Micromass® Q-TOF 2 mass spectrometer
- Ultraviolet-visible (UV-Vis) spectra were obtained at 25 °C using 1 x 1 cm quartz optical cells and recorded on a Shimadzu UV-2501 PC spectrophotometer using dimethylformamide (DMF) as solvent.
- Emission spectra were obtained at HORIBA-Jobin-Yvon Fluoromax 3 spectrofluorometer, at 20°C in DMF using quartz cuvettes 1 x 1 cm.
- The generation of iodine (I₂) was monitored by measuring the iodine absorbance at 340 nm at different pre-defined irradiation times in a Synergy™ HTX Multi-Mode Microplate Reader from BioTek Instruments.
- White light was delivered by a LED system with an irradiance of 25mW.cm².

3.2 METHODS

3.2.1 TPFPP Synthesis (first method)

The first essential molecule to be synthesized is 5,10,15,20-tetrakis(pentafluorophenyl)porphyrin, which is the starting structure that it's going to be conjugated with DBU and DBN.

Rocha Gonsalve's approach (Nitrobenzene Method, figure 3.2.1), was the first method that I used to synthesize TPFPP

The reaction consists in the condensation and cyclization of Pyrrole and pentafluorobenzaldehyde, in stoichiometric proportion 1:1, and the subsequent oxidation of the macrocycle. The oxidative acidic conditions were created by acetic acid and nitrobenzene, and the solution was heated at reflux for 1 h. Distillation was implemented to remove nitrobenzene and subsequently filtration, with progressively more polar eluents, was used to extract TPFPP. A mixture of dichloromethane: methanol 1:3 was added to the filtration product to crystallize TPFPP and remove all the impurities left.

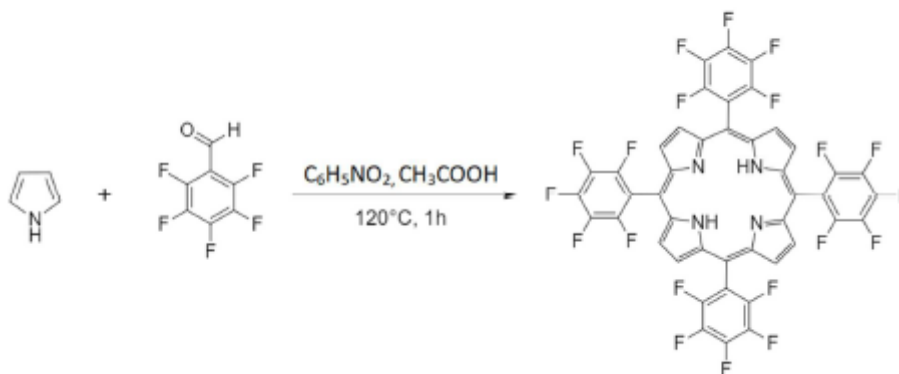


Figure 3.2.1 Rocha Gonsalve's synthesis approach

	n(mmol)	m(g)	V(ml)	d	b.p (boiling point °C)
Pentafluoro Benzaldehyde (PFB)	57,65	11,30	7,2		
Acetic acid			150		151
nitrobenzene			70		
Pyrrol	57,65	3,86	4		

Yield:

Mass TPFPP=0,56 g

Yield= 5%

3.2.2 TPFPP Synthesis (second method)

The second time I had to synthesize TPFPP I used Lindsey synthesis route. It involved the use of a Lewis acid as catalyst to form the porphyrinogen, later oxidized by the addition of an oxidant. In this synthetic route, aldehyde (PFB) and pyrrole were dissolved in dichloromethane (DCM). Due to its sensitivity to the presence of oxygen, the reaction was carried out under inert atmosphere. The solution was then treated with BF₃-Et₂O complex (Lewis acid catalyst) in a ratio that varies between 10 % and 30 %. The catalyst led to the formation of the porphyrinogen, that had to be oxidized by the addition of chloranil to obtain the desired porphyrin. The reaction was done under reflux, at 60°C for 15h.

The resulting solution was then washed with NaHCO₃ solution, filtrated through silica using a 4:1 hexane/DM solution and crystalized using a 2:1 Methane/DM solution.

	n(mmol)	m(g)	V(ml)	D	b.p (boiling point)
2,3,4,5,6–pentafluorobenzaldehyde (PFB)	12,7	2,5			
Pyrrole	14,4	0,966	1		
CH ₂ Cl ₂ (DCM)			600		39.9°C
BF ₃ . Et ₂ OH	4		0,5		
Chloranil	14	3,5			

Yield:

Mass TPFPP=0,861g

Yield= 34,44%

3.2.3 Solvent Selection

Before doing a proper conjugation synthesis between DBU/DBN and TPFPP, I was given the task to find the best solvent in which to conduct the reaction.

The synthesis has been conducted in toluene, chloroform, ethanol, THF, acetonitrile, DMSO and DMF. Ideally the best solvent must either promote the reaction taking place in it, or not interfere at all. All the reactions were made using a 13:1 DBU: TPFPP ratio. The two reagents were put in a round bottom flask, with the appropriate solvent to test, and kept for 1hr at 120°C under reflux.

The products were monitored using TLC, purified using L/L separation and the different phases were separated using preparatory TLC. Each extracted phase underwent ¹HNMR and ¹⁹FNMR to see if the conjugation happened, and its degree.

General procedure

In a two necks round bottom flask of adequate volume, add TPFPP, DBU and the solvent to analyze, under stirring (use ultrasound to help the dissolution). Put the solution in an oil bath at the solvent reflux temperature (don't go over 120°C). After 1h check the solution using an analytical thin layer chromatography (TLC) with eluent 97:3 dichloromethane: methanol. If some products have been produced, vacuum dry the solution. Solubilize the solid in dichloromethane and put the solution in a L/L separation funnel. Add water, stir the two phases, and get the organic phase in a new flask. Make a preparative TLC using a 2%MeOH and 98%DM eluent solution. Scrap the different phases and extract them from silica using 3%MeOH and 97%DM eluent solution.

Non polar Solvents

Synthesis of different conjugates between TPFPP and DBU in Toluene

	n(mmol)	m(mg)	V(ml)	d	b.p (boiling point)
DBU	13,39	2,038	20 E-3		
TPFPP	10,3 E-3	10			
Toluene			1		110,6°C

Toluene produced mainly compound **4** and **5** (see chapter 3.2.5)

The yield was lower than in acetonitrile.

Synthesis of different conjugates between TPFPP and DBU in Cloroform

	n(mmol)	m(mg)	V(ml)	d	b.p (boiling point)
DBU	13,39	2,038	20 E-3		
TPFPP	10,3 E-3	10			
Chloroform			1		61,2°C

TLC showed that most of the starting material didn't react. Only compound **1** was produced, but in small amount.

Polar protic

Synthesis of different conjugates between TPFPP and DBU in Ethanol

	n(mmol)	m(mg)	V(ml)	d	b.p (boiling point)
DBU	13,39	2,038	20 E-3		
TPFPP	10,3 E-3	10			
Ethanol			1		78,37°C

Ethanol seemed initially good because all the substitutions were produced (especially **1**)

Unfortunately, ethanol itself was able to react with TPFPP, competing with DBU in a non-controllable way, thanks to its OH group.

Polar aprotic

Synthesis of different conjugates between TPFPP and DBU in THF

	n(mmol)	m(mg)	V(ml)	d	b.p (boiling point)
DBU	13,39	2,038	20 E-3		
TPFPP	10,3 E-3	10			
THF			1		66°C

The reaction produced all the possible substitutions as confirmed by HNMR and FNMR.

Tetra and trisubstituted were the most common while both disubstituted were not very abundant.

Monosubstituted was produced in very little amount.

Almost no TPFPP remained after the reaction.

Overall, this reaction is good to produce all the compounds.

Synthesis of different conjugate between TPFPP and DBU in acetonitrile

	n(mmol)	m(mg)	V(ml)	d	b.p (boiling point)
DBU	13,39	2,038	20 E-3		
TPFPP	10,3 E-3	10			
Acetonitrile			1		82°C

In acetonitrile all the substituents were formed, and it didn't interact in any way with the reagents. Before making a TLC, acetonitrile must be completely removed, otherwise it will interfere with the elution and separation of the products.

Synthesis of different conjugate between TPFPP and DBU in DMF

	n(mmol)	m(mg)	V(ml)	d	b.p (boiling point)
DBU	13,39	2,038	20 E-3		
TPFPP	10,3 E-3	10			
DMF			1		153°C

In DMF there was a precipitation. The solvent reacted with TPFPP.

This was confirmed by the solid, as ¹⁹FNMR showed that all the F atoms disappeared.

Almost all TPFPP was consumed.

Overall conclusions:

All the reactions (except the one in chloroform) produced compound **5**.

Compound **1** was produced in THF, ethanol, acetonitrile and chloroform only.

THF is not accepted as a good solvent to make molecules with medical application, as it's a class 1 compound in the ICH guidelines, so it won't be used in further studies.

DMF and ethanol had to be avoided, as they react with TPFPP.

NMP was used too after these studies, but it was not used as main solvent, as it was really difficult to remove, it disturbed the TLCs and didn't have better yields compared to acetonitrile. It was used in OHMIC reaction as it mixes with water.

Acetonitrile was the only one with less issues, and in which it was possible to produce all the substitutions.



3. from left to right, TLCs of the various reactions using different solvents: toluene, THF, acetonitrile, DMF, ethanol, chloroform and ethanol (specific)

3.2.4 OHMIC reactions

The aim of this synthesis method was to try to make a conjugation reaction of an insoluble porphyrin and a base in water.

The first attempt, using only water as solvent, had no results.

In a successive attempt, NMP was added to water and some product was formed.

Brine was added to the water solution (40 drops), increasing the conductivity, and increasing the product.

After several attempts I could see clear results from TLC.

Synthesis using OHMIC is possible if NMP and brine is added.

As this was a side project it was not optimized any further, but there were some results, and this could be a viable approach if optimized. The main issue remains how to remove completely and fast NMP.

3.2.5 General procedure to synthesize TPFPP+DBU compounds

In two necks round bottom flask of adequate volume, add TPFPP (200 mg, 0,206mmol, 1equiv) in Acetonitrile (30ml) under stirring (use ultrasound to help the dissolution). At the same time prepare the DBU solution (300µl, 2,678 mmol, 13equiv) in acetonitrile (2.7ml) and put it in a syringe. Put the syringe in the syringe pump and set the parameters to V= 3ml and speed of 3 ml/hr. Put the TPFPP solution in an oil bath at 120°C and, when it's refluxing, press start on the syringe pump. After 1h check the solution every 15 minutes using an analytical thin layer chromatography (TLC) with eluent 97/3 dichloromethane/methanol, until you are satisfied with the results. Vacuum dry the solution. Solubilize the solid in dichloromethane and put the solution in a separation funnel. Add water, stir the two phases, and get the organic phase in a new flask. Make a preparative TLC using a 4%MeOH and 96%DM eluent solution. Scrap the different phases and extract them from silica using 4%MeOH and 96%DM eluent solution or acetic acid or acetone.

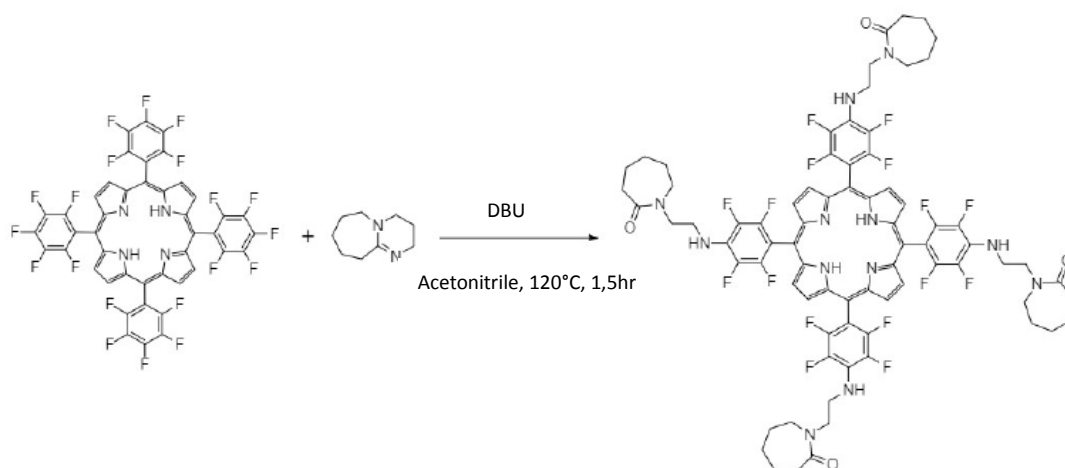


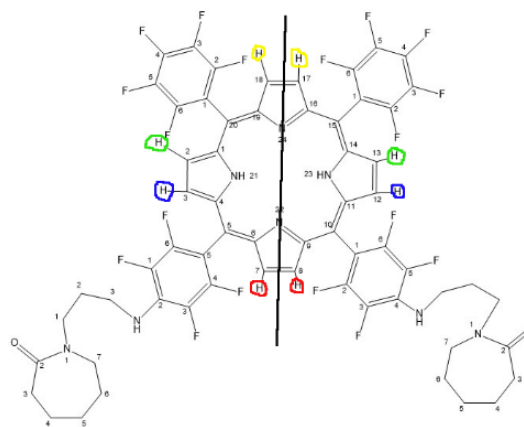
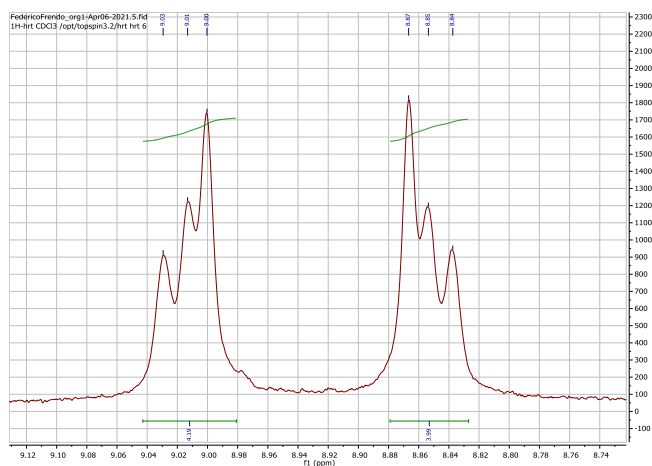
Figure 3.2.5a reaction between TPFPP and DBU, forming compound 5

TPFPP+DBU monosubstituted (compound 1)

The synthesis of TPFPP+DBU monosubstituted was carried out by following the general procedure. This compound was separated from the others using preparative silica TLC (fifth band from baseline) and extracted using acetic acid, giving 21,73mg (19,32 μ mol; 9,42% yield). ^1H NMR (CDCl_3) δ ppm: 8,97(m, 8H, H n10);5,54 (s, 1H, H n9);3,51 (dt, J=6,2, 4H, H n1,3);3,14 (m, 2H, H n4);2,52 (m, 2H, H n6) ;1,78 (m, 2H, H n3);1,65(ddd, J=5,9Hz, 4H, H n5,7);1,48 (m, 2H, H n8); -2,90 (s,2H, H n11). ^{13}C NMR (CDCl_3) δ ppm:128,85 (C n10); 49,39 (C 4) ; 45,07(C n3); 41,76 (C n1); 37,95 (C n6); 30,32 (C n5); 28,82(C n2); 28,32 (C n8); 23,60 (C n7). MS: m/z: 1125,4 (fig.3.2.5a)

TPFPP+DBU disubstituted trans (compound 2)

The synthesis of TPFPP+DBU disubstituted trans was carried out by following the general procedure. This compound was separated from the others using preparative silica TLC (fourth band from baseline) and extracted using Pure acetone, giving 10,46mg (8,21 μ mol; 4% yield). ^1H NMR (CDCl_3) δ ppm: 8,94(dd, J=4,8Hz, 8H, H n11);5,68 (s, 2H, H n9);3,65 (d, J=6,3Hz, 8H, H n1,3);3,39 (m, 4H, H n4);2,63 (m, 4H, H n6) ;1,94 (m, 4H, H n3);1,77(m, 8H, H n7,5);1,69 (p,J=5,2Hz, 4H, H n8); -2,87 (s,2H, H n11). ^{13}C NMR (CDCl_3) δ ppm:129,42(C n10); 44,84(C n3); 49,60(C n4); 41,52(C n1); 36,92(C n6); 29,91(C n5); 28,62(C n2); 28,43(C n8); 23,46(C n7). MS: m/z: 1275,5 (fig.3.2.5a)

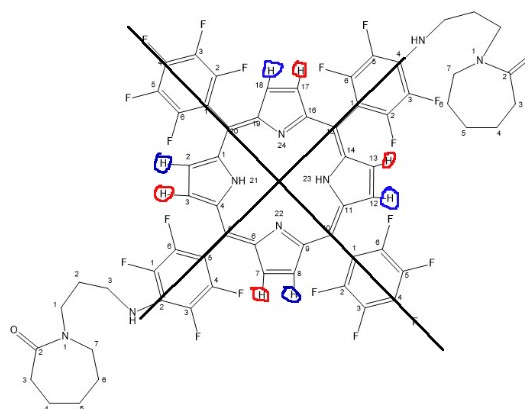
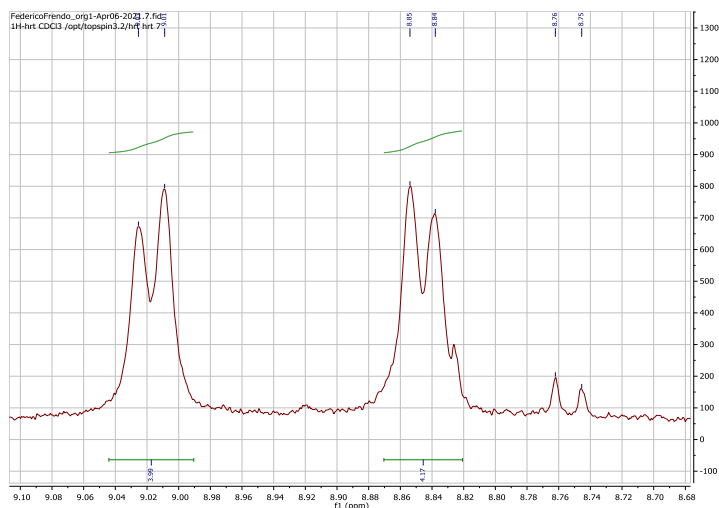


Cis and Trans substitution have the same spectra. The only way to differentiate them is by looking at the shape of the signals at 8,94 δ ppm (porphyrinic H). For the Trans compound it's possible to see 6 peaks divided in two symmetrical couples of 3 peaks each. That's because there is only one plain of symmetry in the trans molecule, making at least 3 H atoms different in the pyrrolic ring. The same applies to compound 7.

TPFPP+DBU disubstituted cis (compound 3)

The synthesis of TPFPP+DBU disubstituted cis was carried out by following the general procedure. This compound was separated from the others using preparative silica TLC (third band from baseline) and extracted using Pure acetone, giving 17,32mg of compound (13,58 μmol ; 6,62% yield).

^1H NMR (CDCl_3) δ ppm: 8,94(m, 8H, H n10); 5,65 (s, 2H, H n9); 3,62 (d, J=6,2Hz, 8H, H n1,3); 3,34 (m, 4H, H n4); 2,60 (t, J=5,2Hz, 4H, H n6); 1,91 (t, J=6,2Hz, 4H, H n3); 1,75(m, 8H, H n7,5); 1,65 (s, 8H, H n8); -2,87 (s, 2H, H n11). ^{13}C NMR (CDCl_3) δ ppm: 129,28(C n10); 49,55(C n4); 45,03(C n3); 41,69(C n1); 36,92(C n6); 29,91(C n5); 28,62 (C n3); 28,43(C n2); 23,46(C n7). MS: m/z: 1275,4 (fig.3.2.5a)



Cis and trans substitution have the same spectra. The only way to differentiate them is by looking at the shape of the signals at 8,94 δ ppm. For the cis compound it's possible to see 4 peaks divided in two symmetrical couples of 2 peaks. That's because there are two planes of symmetry in the trans molecule, making only two H atoms differ between them in the pyrrolic ring. The same applies to compound 8.

TPFPP+DBU Trisubstituted (compound 4)

The synthesis of TPFPP+DBU tetrasubstituted was carried out by following the general procedure. This compound was separated from the others using preparative silica TLC (second band from baseline) and extracted using Pure acetone, giving 52,6mg of compound (36,95 μmol ; 18% yield).

NMR (CDCl_3) δ ppm: 8,92(m, 8H, H n10); 5,60 (s, 3H, n9); 3,58 (d, J=6,7Hz; 12H, H n1,3); 3,26 (m, 6H, H n4); 2,57 (dd, J=3,6Hz, 6H, H n5); 1,87 (t, J= 6,2Hz, 6H, H n3); 1,70(dd, J= 3,1Hz, 12H, H n7,5); 1,75 (dd, J= 3,2Hz, 6H, H n8); -2,87 (s, 2H, H n11). ^{13}C NMR (CDCl_3) δ ppm: 129,15 (C n10); 49,57(C n4); 44,86(C n3); 41,65(C n1); 37,10(C n6); 29,97(C n5); 28,73(C n2); 28,34(C n8); 23,37(C n7). MS: m/z: 1425,6 (fig.3.2.5a)

TPFPP+DBU tetrasubstituted (compound 5)

The synthesis of TPFPP+DBU tetrasubstituted was carried out by following the general procedure. This compound was separated from the others using preparative silica TLC (first band from baseline) and extracted using Pure acetone, giving 42,84 mg of compound (27,2 μmol , 21,42% yield). ^1H NMR (CDCl_3) δ ppm: 8,99(s, 8H, H-porphyrin ring);5,54 (s, 4H, H-N);3,51 (m, 16H, H propane chain);3,14 (m, 8H, H close to N in aliphatic ring);2,52 (m, 8H, H in aliphatic ring) ;1,78 (t, J= 6,2Hz, 8H, H mid propane chain);1,65(m, 17H, H in aliphatic ring);1,48 (m, 7H, H close to O in aliphatic ring); -2,98 (s,2H, H-N porphyrin ring). ^{13}C NMR (CDCl_3) δ ppm:128,85(C n10); 49,39(C n4); 45,07(C n3); 41,76(C n1); 37,95(C n6); 30,32(C n5); 28,82(C n2); 28,32(C n8); 23,60 (C n7). MS: m/z: 1576,8 (fig.3.2.5a)

Reaction	TPFPP (start)	TPFPP(left)	Mono	Disub trans	Disub cis	Trisub	Tetrasub	Tot.
AN+DBU 4hrs	200mg	-	9,42% (21,73mg; 19,32 μmol)	4% (10,46mg; 8,21 μmol)	6,62% (17,32mg; 13,58 μmol)	18% (52,6mg; 36,95 μmol)	15% (48,53mg; 30,8 μmol)	53,04%

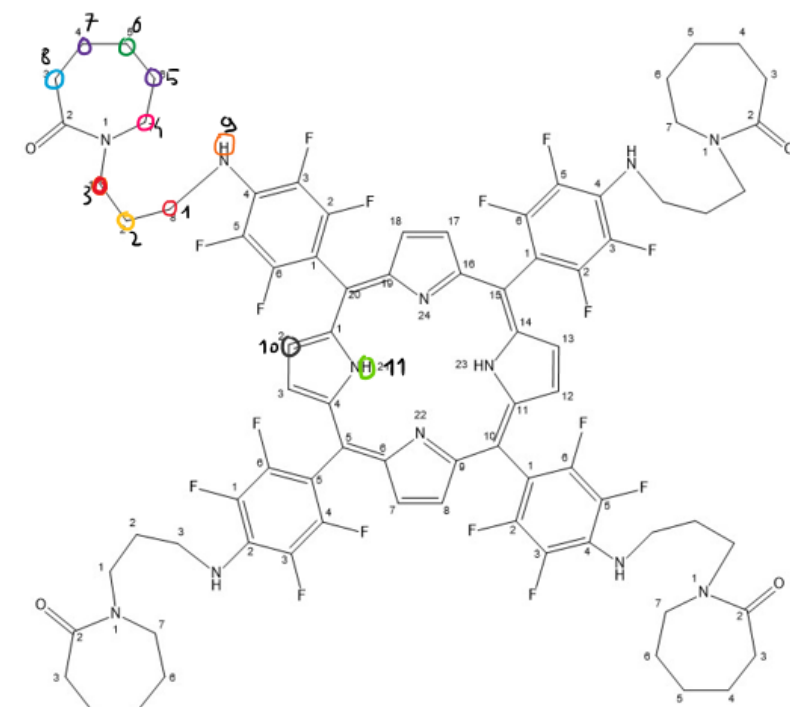


Figure 3.2.5b Picture that correlates the C atoms with their signal

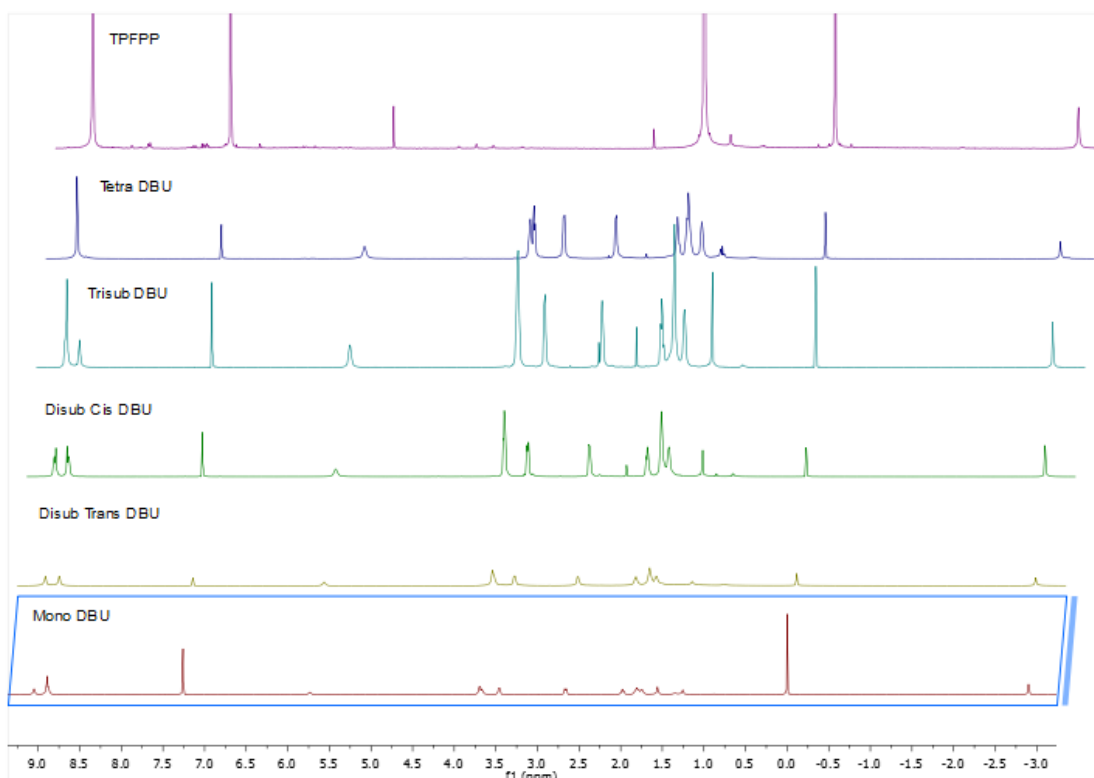


Figure 3.2.5c ^1H NMR comparison between DBU compounds. From top to bottom: TPFPF, Tetrasubstituted DBU, Trisubstituted DBU, Disubstituted Cis DBU, Disubstituted Trans DBU, Monosubstituted DBU

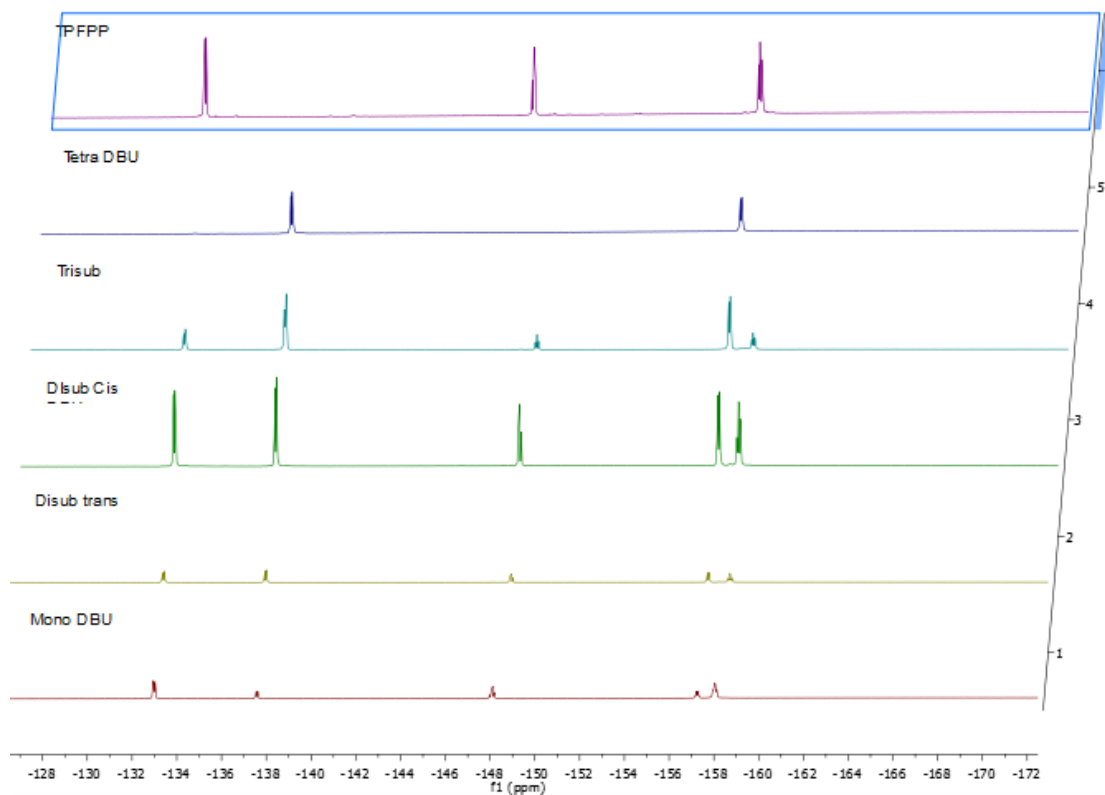


Figure 3.2.5d ^{13}C NMR comparison between DBU compounds. From top to bottom: TPFPF, Tetrasubstituted DBU, Trisubstituted DBU, Disubstituted Cis DBU, Disubstituted Trans DBU, Monosubstituted DBU

3.2.6 General procedure to synthesize TPFPP+DBN compounds

In a two necks round bottom flask with of adequate volume, add 200 mg of TPFPP and 30 ml of Acetonitrile under stirring (use ultrasound to help the dissolution). At the same time prepare a 6ml solution of DBU (400 μ l = 407,6mg) and acetonitrile (5.6ml) and put it in a syringe. Put the syringe in the syringe pump and set the parameters to V= 6ml and speed at 6 ml/hr. Put the TPFPP solution in an oil bath at 85°C and, when it's refluxing, press start on the syringe pump. After 1h check the solution every 15 minutes using an analytical thin layer chromatography (TLC) with eluent 97/3 dichloromethane/methanol, until you are satisfied with the results. Vacuum dry the solution. Solubilize the solid in dichloromethane and put the solution in a separation funnel. Add water, stir the two phases, and get the organic phase in a new flask. Make a preparative TLC using a 4%MeOH and 96%DM eluent solution. Scrap the different phases and extract them from silica using 4%MeOH and 96%DM eluent solution or acetic acid or acetone.

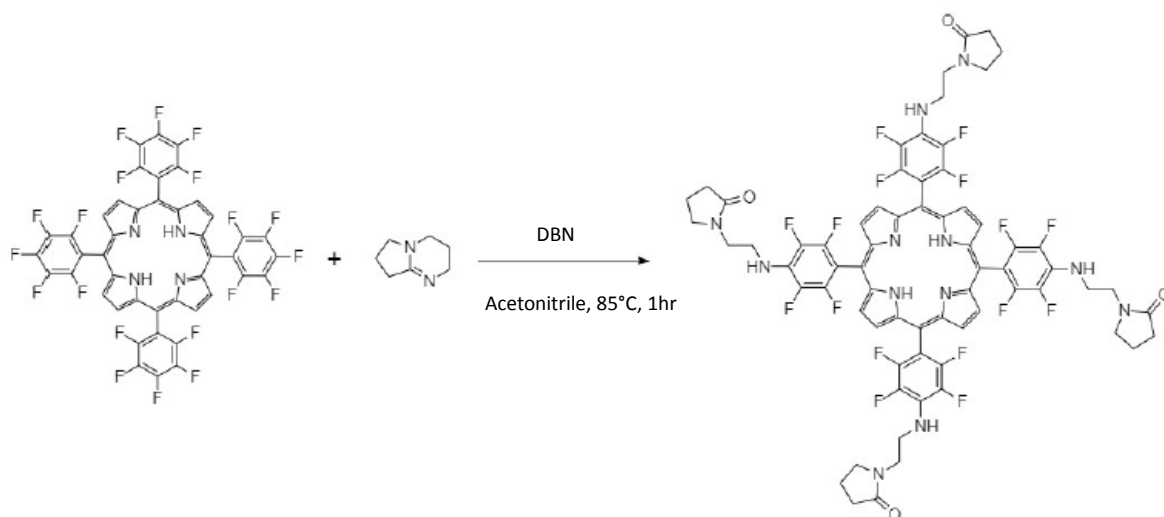


Figure 3.2.6a reaction between TPFPP and DBN, forming compound 10

TPFPP+DBN monosubstituted (compound 6)

The synthesis of TPFPP+DBN monosubstituted was carried out by following the general procedure. This compound was separated from the others using preparative silica TLC (fifth band from baseline) and extracted using Pure acetone, giving 52,4mg of compound (47,7 μ mol, 23,3% yield). ^1H NMR (CDCl_3) δ ppm: 8,95(s, 8H, H-porphyrin ring);5,25 (s, 1H, H-N);3,67 (s, 2H, H propane chain near N in aliphatic ring);3,60 (t, J=6,3Hz 2H, H propane chain near NH);3,52 (t, J=7,1Hz, 2H, H in aliphatic ring close to N in aliphatic ring) ;2,52 (t, J= 8,1Hz, 2H, H in aliphatic ring);2,14(m, 2H, H close to O in aliphatic ring);2,01 (p, J=6,3Hz 2H, H mid propane chain); -2,98 (s,2H, H-N porphyrin ring). ^{13}C NMR (CDCl_3) δ ppm:131,6(C n8); 47,38(C n4); 42,02(C n3); 39,13(C n1); 31,05 (C n6); 28,05(C n2); 17,78 (C n5). MS: m/z: 1096,16

TPFPP+DBN disubstituted trans (compound 7)

The synthesis of TPFPP+DBN disubstituted trans was carried out by following the general procedure. This compound was separated from the others using preparative silica TLC (fourth band from baseline) and extracted using Pure acetone, giving 12mg of compound (9,85 μ mol, 4,80% yield).

^1H NMR (CDCl_3) δ ppm: 8,95(s, 8H, H-porphyrin ring);5,25 (s, 2H, H-N);3,68 (d, $J=6,4\text{Hz}$, 4H, H propane chain near N in aliphatic ring);3,58 (t, $J=6,4\text{Hz}$ 4H, H propane chain near NH);3,52 (t, $J=7,0\text{Hz}$, 4H, H in aliphatic ring close to N in aliphatic ring) ;2,53 (t, $J= 8,1\text{Hz}$, 4H, H in aliphatic ring);2,13(m, 4H, H close to O in aliphatic ring);2,02 (p, $J=6,3\text{Hz}$ 4H, H mid propane chain); -2,98 (s,2H, H-N porphyrin ring). ^{13}C NMR (CDCl_3) δ ppm:130,75(C n8); 47,48(C n4); 41,76(C n3); 39,35(C n1); 30,32 (C n6); 27,92(C n2); 17,88 (C n5). MS: m/z: 1218,27

TPFPP+DBN disubstituted cis (compound 8)

The synthesis of TPFPP+DBN disubstituted cis was carried out by following the general procedure. This compound was separated from the others using preparative silica TLC (third band from baseline) and extracted using Pure acetone, giving 24,4 mg of compound (20,28 μ mol, 9,88% yield).

^1H NMR (CDCl_3) δ ppm: 8,95(s, 8H, H-porphyrin ring);5,25 (s, 4H, H-N); 3,67 (t, $J=6,5\text{Hz}$, 4H, H propane chain near N in aliphatic ring);3,60 (t, $J=6,3\text{Hz}$ 4H, H propane chain near NH);3,52 (t, $J=7,1\text{Hz}$, 4H, H in aliphatic ring close to N in aliphatic ring) ;2,52 (t, $J= 8,1\text{Hz}$, 4H, H in aliphatic ring);2,14 (m, 4H, H close to O in aliphatic ring);2,01 (t, $J=6,1\text{Hz}$ 4H, H mid propane chain); -2,98 (s,2H, H-N porphyrin ring). ^{13}C NMR (CDCl_3) δ ppm:131,85(C n8); 47,38(C n4); 42,24(C n3); 39,52(C n1); 30,90 (C n6); 28,18(C n2); 18,10 (C n5). MS: m/z: 1218,27

TPFPP+DBN Trisubstituted (compound 9)

The synthesis of TPFPP+DBN trisubstituted was carried out by following the general procedure, but using 125mg of TPFPP and 7 equivalents of DBN instead. This compound was separated from the others using preparative silica TLC (second band from baseline) and extracted using Pure acetone, giving 36,06mg of compound (51,4 μ mol, 28% yield). ^1H NMR (CDCl_3) δ ppm: 8,95(s, 8H, H-porphyrin ring);5,25 (s, 3H, H-N);3,66 (d, $J=6,9\text{Hz}$, 6H, H propane chain near N in aliphatic ring);3,58 (m, 6H, H propane chain near NH);3,49 (m, 6H, H in aliphatic ring close to N in aliphatic ring) ;2,51 (dd, $J= 9,7;6,5\text{Hz}$, 6H, H in aliphatic ring);2,13(t, $j=7,8\text{Hz}$, 6H, H close to O in aliphatic ring);2,00 (m, 6H, H mid propane chain); -2,98 (s,2H, H-N porphyrin ring). ^{13}C NMR (CDCl_3) δ ppm:131,85(C n8); 47,38(C n4); 42,24(C n3); 39,52(C n1); 30,90 (C n6); 28,18(C n2); 18,10 (C n5). MS: m/z: 1340,37

TPFPP+DBN Tetrasubstituted (compound 10)

The synthesis of TPFPP+DBN tetrasubstituted was carried out by following the general procedure, but using 125mg of TPFPP and 7 equivalents of DBN instead. This compound was separated from the others using preparative silica TLC (first band from baseline) and extracted using Pure acetone, giving 62,9 mg of compound (39,92 μ mol, 31% yield). ^1H NMR (CDCl_3) δ ppm: 8,95(s, 8H, H-porphyrin ring); 5,25 (s, 4H, H-N); 3,65 (t, J=6,5Hz, 8H, H propane chain near N in aliphatic ring); 3,58 (t, J=6,5Hz 8H, H propane chain near NH); 3,50 (t, J=7,1Hz, 8H, H in aliphatic ring close to N in aliphatic ring); 2,51 (t, J= 8,0Hz, 8H, H in aliphatic ring); 2,13(p, j=7,6Hz, 8H, H close to O in aliphatic ring); 2,00 (p, J=6,4Hz 8H, H mid propane chain); -2,98 (s, 2H, H-N porphyrin ring). ^{13}C NMR (CDCl_3) δ ppm: 131,85(C n8); 47,38(C n4); 42,24(C n3); 39,52(C n1); 30,90 (C n6); 28,18(C n2); 18,10 (C n5). MS: m/z: 1462,48

Reaction	TPFPP (start)	TPFPP(left)	Mono	Disub trans	Disub cis	Trisub	Tetrasub	Tot.
AN+DBN 7 equiv	125mg	-	4,21% (6,1mg; 5,42 μ mol)	3,21% (5,3 mg; 4,16 μ mol)	2,55% (4,2mg; 3,29 μ mol)	28% (51,4 mg; 36,06 μ mol)	31% (62,9mg; 39,92 μ mol)	68,97%
AN+DBN 5 equiv	200mg	30%	23,3% (52,4mg; 47,7 μ mol)	4,80% (12mg; 9,85 μ mol)	9,88% (24,4mg; 20,28 μ mol)	6,87% (18,8mg; 14,1 μ mol)	4,53% (13,6mg; 9,3 μ mol)	49,38%

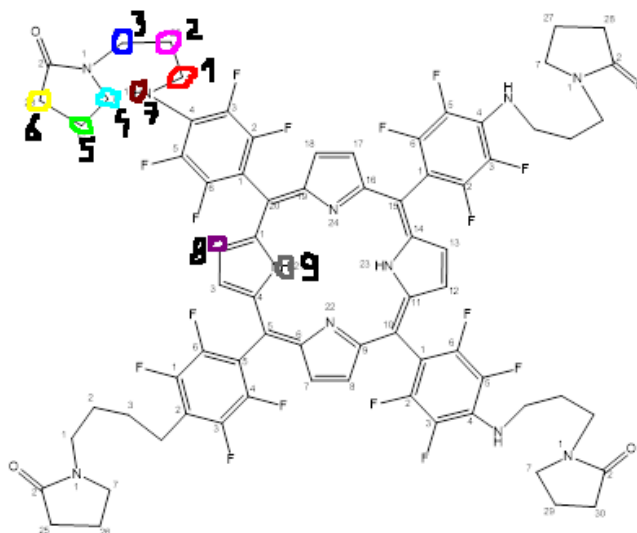


Figure 3.2.6b Picture that correlates the C atoms with their signal

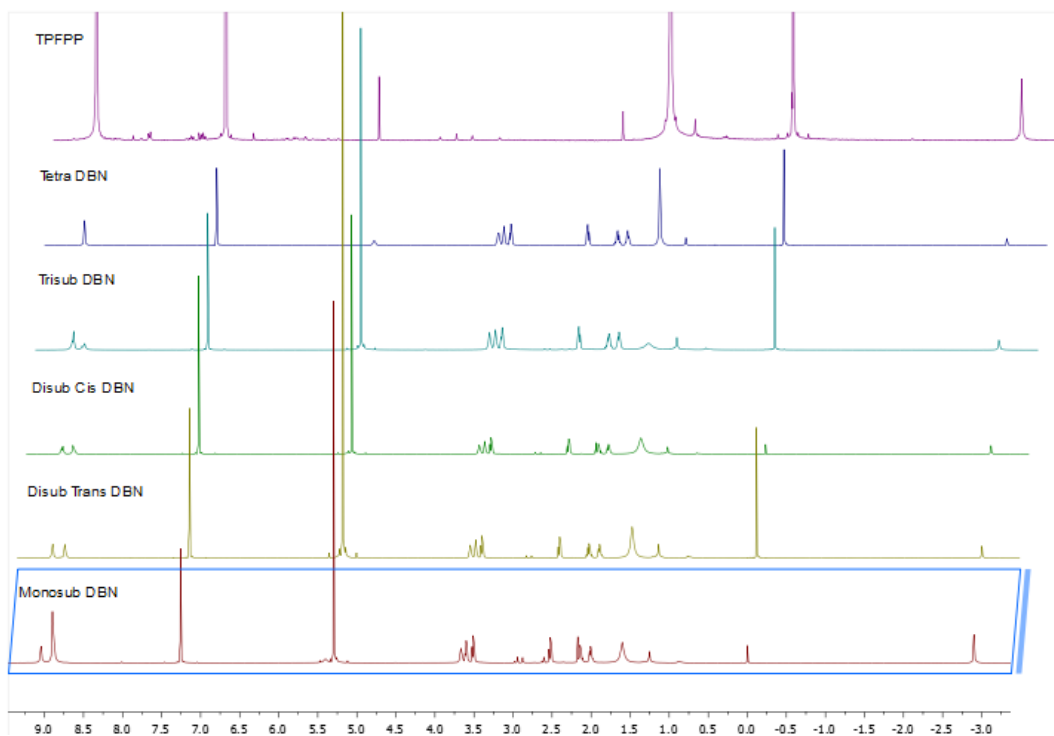


Figure 3.2.6c ^1H NMR comparison between DBN compounds. From top to bottom: TPFPP, Tetrasubstituted DBN, Trisubstituted DBN, Disubstituted Cis DBN, Disubstituted Trans DBN, Monosubstituted DBN

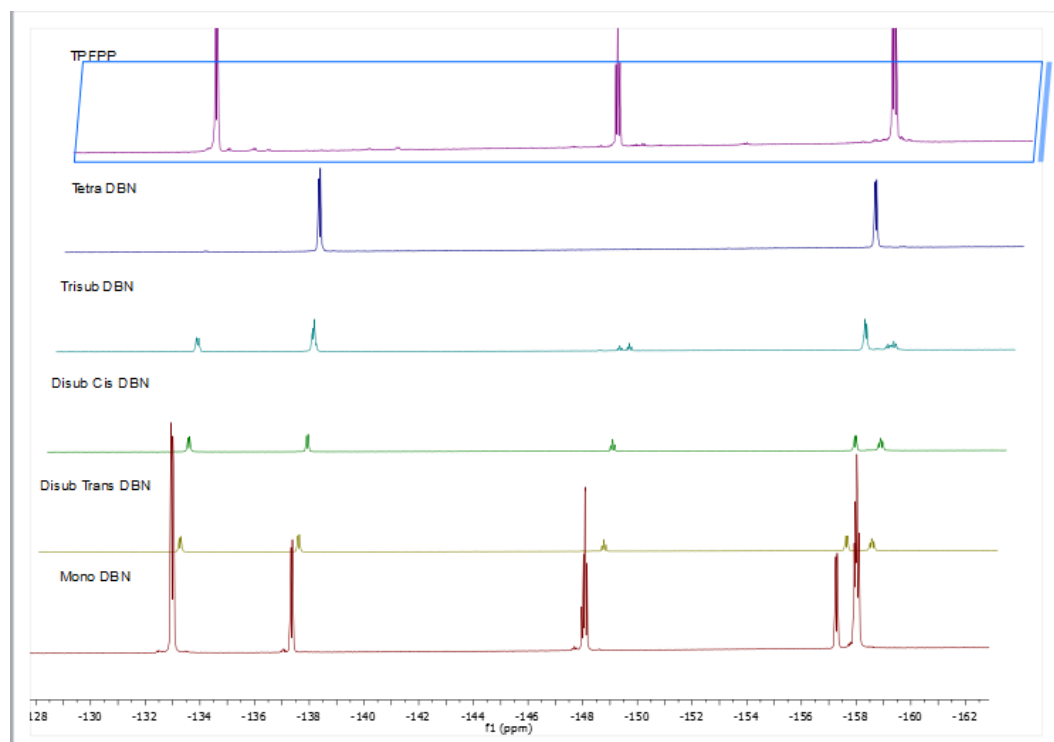


Figure 3.2.6d ^{13}C NMR comparison between DBN compounds. From top to bottom: TPFPP, Tetrasubstituted DBN, Trisubstituted DBN, Disubstituted Cis DBN, Disubstituted Trans DBN, Monosubstituted DBN

3.3 Photophysical results

3.3.1 Fluorimetry

The absorption spectra were obtained in a HORIBA-Jobin-Yvon Fluoromax 3 spectrofluorometer, at 20° C in DMF using quartz cuvettes 1 x 1 cm. Each absorption spectrum was registered for the compound and the TPP (reference).

The emission spectra were acquired after excitation at a precise wavelength, which corresponds to the wavelength where the absorption spectra of TPP (reference) and the new compound were matching. Fluorescence quantum yield is calculated using the following equation,

$$\Phi_F = \Phi_F^{Std} \frac{A}{A_{Std}}$$

where Φ^{Std} is the fluorescence quantum yield of the TPP (reference) and A and A_{Std} correspond to the areas of the fluorescence spectra of the compound and reference, respectively.

General procedure

Using an UV spectrometry machine make the baseline using DMF as solvent of choice. Add a small amount of TPP (standard) into a quartz vial and elute it with DMF. Run the UV spectra. Fix the wavelength at 417nm and dilute the solution until you have 0,2Å, then take 1ml of this solution and put it in a 10ml volumetric flask. Fill the volumetric flask with DMF to get a 0,02Å solution. Use this solution to get the fluorimeter spectra using the following settings: excitation 416nm, slit 2nm; emission wavelength starts 620nm, end 800nm, slit 2nm.

Compound	Integrated Area	Quantum Yield
TPP	1581561	0,11
Mono DBU	635451	0,044
Disub T DBU	729568	0,051
Disub C DBU	688863	0,048
Trisub DBU	806616	0,056
Tetra DBU	881718	0,061
Tetra DBN	840247	0,058

Table 3.3.2a fluorescence data for TPFPP+DBU and TPFPP+DBN tetrasubstituted

Compound	Area	Quantum Yield
TPP	1432113	0,11
Mono DBN	799158	0,061
Disub T DBN	1076015	0,083
Disub C DBN	703287	0,054
Trisub DBN	774437	0,059

Table 3.3.2b fluorescence data for TPFPP+DBN compound series

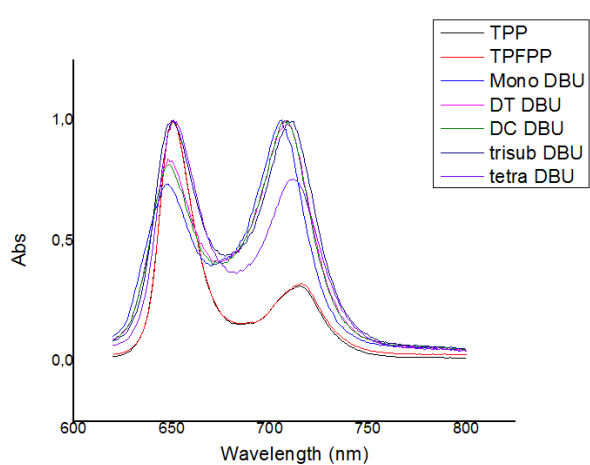


Figure 3.3.2a Fluorescence spectra of TPFPP+ DBU compound series and TPP at 20°C in DMF ($\lambda_{ex} = 417\text{nm}$)

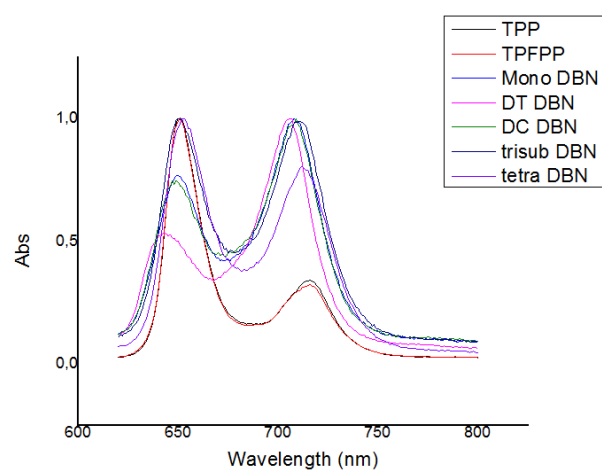


Figure 3.3.2b Fluorescence spectra of TPFPP+ DBN compound series and TPP at 20°C in DMF ($\lambda_{ex} = 417\text{nm}$)

3.3.2 UV spectrometry analysis

Ultraviolet-visible (UV-Vis) spectra were obtained at 25 °C using 1 x 1 cm quartz optical cells and recorded on a Shimadzu UV-2501 PC spectrophotometer using dimethylformamide (DMF) as solvent.

This analysis was made to check the molar absorption coefficient (ϵ) at each peak for each compound. It was calculated by plotting five different A measurement with their corresponding concentration, at a given wavelength, following Lambert Beer equation.

$$\epsilon = \frac{A}{C * b}$$

General procedure

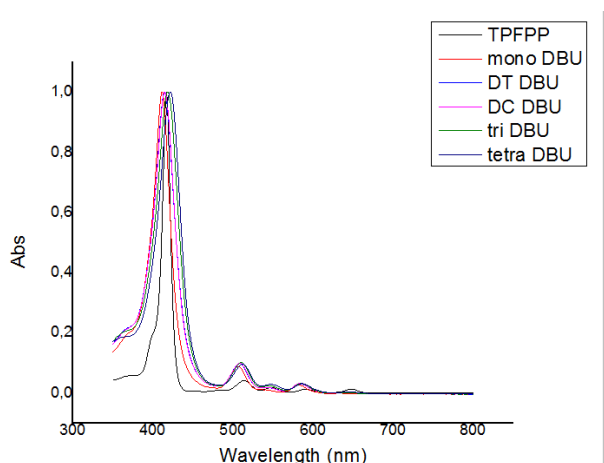
Solubilize the compound in 1ml of DMF and calculate the concentration. Put the right amount of that solution to get a 1E-4 M concentration in 3ml solution. Run an UV spectrum and then remove 300 μ l from this solution and put it in another vial and add 2,7ml of DMF to obtain a 1E-5M solution that you'll use later to determine the Soret band. Add 300 μ l of DMF to the 1E-4 solution and run another spectrum. Remove and add 300 μ l of solution/solvent until you have 5 different measurements. Run a spectrum with the 1E-5M solution and then remove 200 μ l of this solution and add 200 μ l of DMF. Repeat this until you have five different spectrums.

ϵ DBU compounds

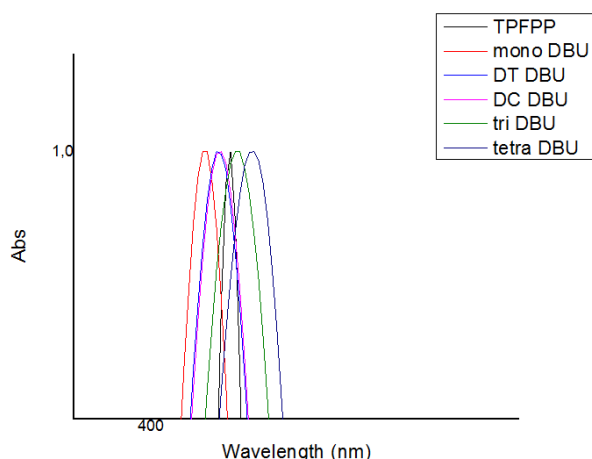
ϵ values are reported in log scale.

compound	ϵ (410nm) soret	ϵ (505nm) qband1	ϵ (535nm) Shoulder	ϵ (580nm) Qband2	ϵ (640nm) Qband3
Mono	5,3	4,3	3,5	3,7	2,8
Disub T	5,2	4,2	3,5	3,8	2,8
Disub C	5,3	4,3	3,6	3,8	2,9
Trisub	5,3	4,3	3,7	3,8	3,0
Tetrasub DBU	5,4	4,3	3,8	3,9	3,2

Table 3.3.3a Absorption data of TPFPP+DBU compound series (logarithmic values)



Normalized UV-visible absorption spectra of TPFPP+DBU compound series obtained at 20°C in DMF



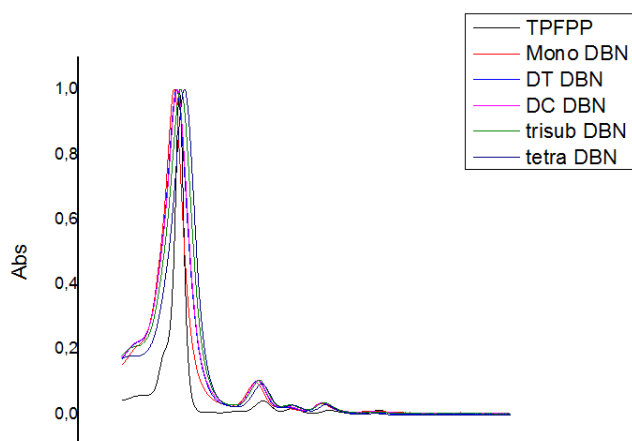
Normalized UV-visible absorption spectra of TPFPP+DBU compound series obtained at 20°C in DMF (Soret band detail)

ϵ DBN compounds

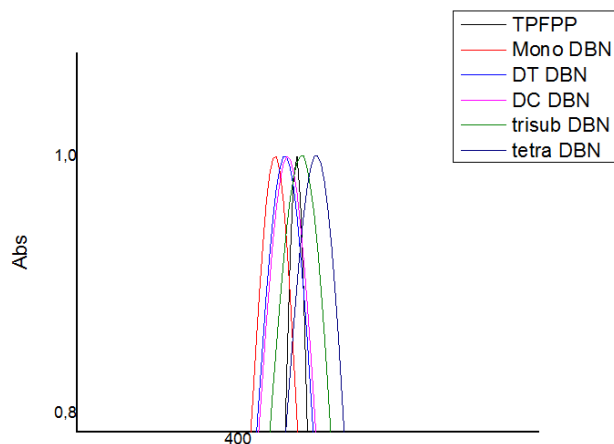
ϵ values are reported in log scale.

compound	$\epsilon(410\text{nm})$ soret	$\epsilon(505\text{nm})$ qband1	$\epsilon(535\text{nm})$ Shoulder	$\epsilon(580\text{nm})$ Qband2	$\epsilon(640\text{nm})$ Qband3
Mono	5,3	4,3	3,6	3,8	3,2
Disub T	5,2	4,3	3,8	3,8	3,0
Disub C	5,2	4,2	3,5	3,7	2,9
Trisub	5,3	4,3	3,8	3,8	3,1
TetrasubDBN	5,4	4,4	3,8	3,8	3,0

table 3.3.3b Absorption data of TPFPP+DBN compound series (logarithmic values)



Normalized UV-visible absorption spectra of TPFPP+DBN compound series obtained at 20°C in DMF



Normalized UV-visible absorption spectra of TPFPP+DBN compound series obtained at 20°C in DMF (Soret band detail)

3.3.3 Singlet Oxygen Generation

DMA Ultraviolet-visible (UV-Vis) spectra were obtained at 25 °C using 1 x 1 cm quartz optical cells and recorded on a Shimadzu UV-2501 PC spectrophotometer.

The light for the controlled singlet oxygen generation was delivered by an HORIBA-Jobin-Yvon Fluoromax 3 spectrofluorometer, at 20° C in DMF using quartz cuvettes 1 x 1 cm.

Quantum yield of singlet oxygen (Φ_{Δ}) is a value that represent how quickly the DMA absorbance value decreases, and so how quickly singlet oxygen is formed. Higher Φ_{Δ} values indicate a good photosensitizer. Φ_{Δ} is calculated by the following equation:

$$\Phi_{\Delta} = \Phi_{\Delta}^{\text{Std}} \frac{k I_{\text{abs}}^{\text{Std}}}{k^{\text{Std}} I_{\text{abs}}}$$

$$\frac{I_{\text{abs}}^{\text{std}}}{I_{\text{abs}}} = \frac{1 - 10^{-A_{660}^{\text{std}}}}{1 - 10^{-A_{660}}}$$

General procedure

Before measuring samples: Run the baseline in the UV spectrometer (DMF as solvent). Put in a vial: 3ml of DMF and 18,9 μ l of DMA (calculated). Run 3 measurements at 378nm and calculate the average absorbance value. Put the vial in the fluorimeter and run the program for a minute. Repeat until you have a total of 11 measurements. Then repeat this procedure for a second time so that you have two sets of 11 measurements each.

For samples: Obtain a 0,2 A solution of your sample at 507nm. Put 18,9 μ l of DMA in the vial. Run 3 measurements at 378nm and calculate the average absorbance value. Put the vial in the fluorimeter and run the program for a minute. Repeat until you have a total of 11 measurements. Then repeat this procedure for a second time so that you have two sets of 11 measurements each.

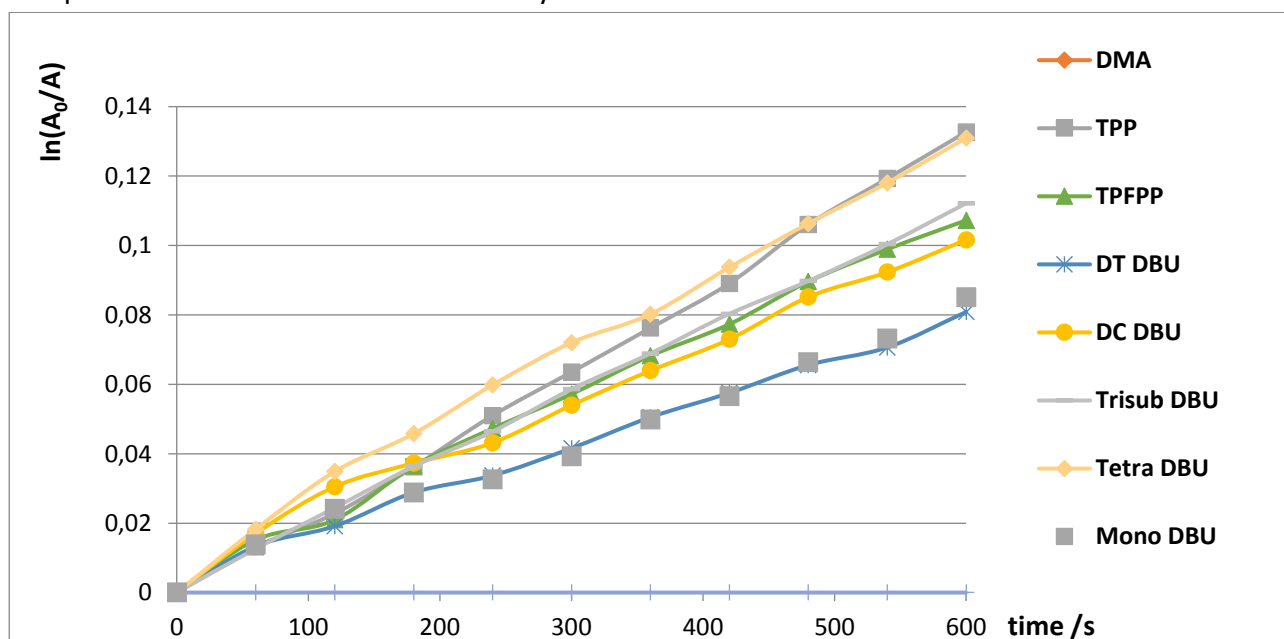


Figure 3.3.4a Graphic depicting the logarithm of the decadence of absorbance of DMA caused by the production of sO radicals for TPFPP+DBU compound series

Abs 507 nm	compound	Istd/I	K	$\phi\Delta$
0,101	TPP	1	2,23E-04	0,65
0,101	TPFPP	1	1,79E-04	0,52
0,101	Mono DBU	1	1,31E-04	0,38
0,1	DT DBU	1,009504	1,28E-04	0,38
0,101	DC DBU	1	1,61E-04	0,47
0,1	trisub DBU	1,009504	1,85E-04	0,54
0,101	tetra DBU	1	2,10E-04	0,61

Table 3.3.4a Data from singlet oxygen test for TPFPP+DBU compound series

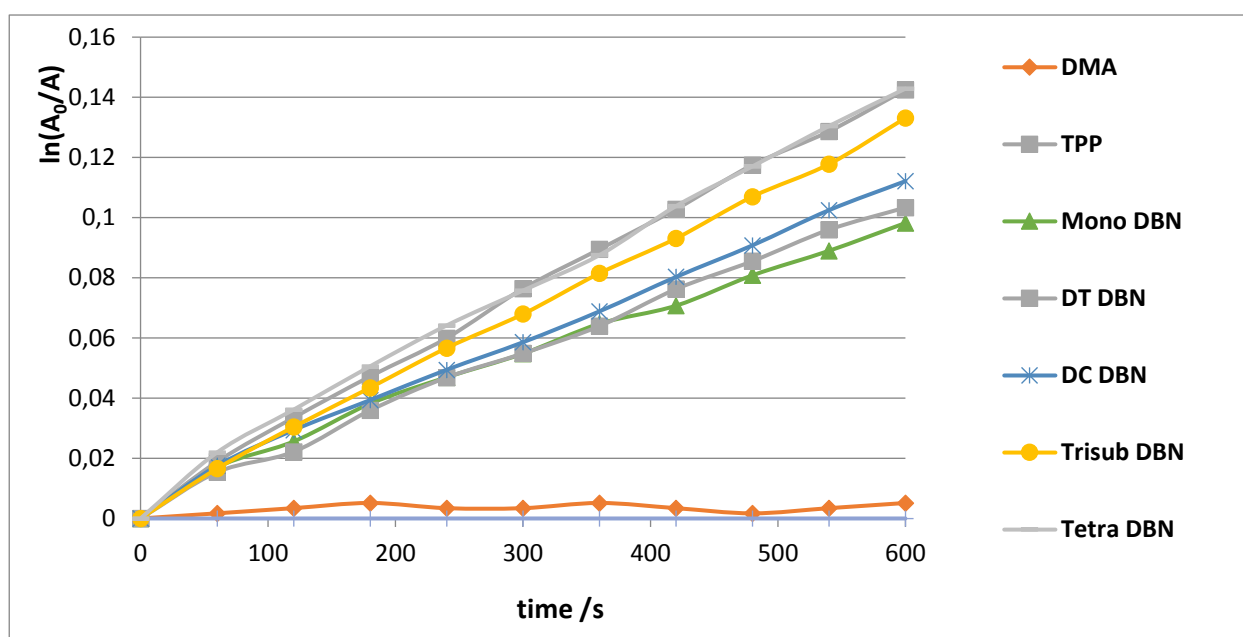


Figure 3.3.4b Graphic depicting the logarithm of the decadence of absorbance of DMA caused by the production of sO radicals for TPFPP+DBN compound series

Abs 507 nm	compound	Istd/I	K	$\phi\Delta$
0,101	TPP	1	2,34E-04	0,65
0,101	Mono DBN	1	1,56E-04	0,43
0,102	DT DBN	0,990683	1,71E-04	0,47
0,102	DC DBN	0,990683	1,80E-04	0,49
0,101	Tri DBN	1	2,16E-04	0,60
0,101	Tetra DBN	1	2,30E-04	0,64

Table 3.3.4b Data from singlet oxygen test for TPFPP+DBN compound series

3.3.4 KI Singlet oxygen generator assay

The generation of iodine (I_2) was monitored by measuring the iodine absorbance at 340 nm at different pre-defined irradiation times in a Synergy™ HTX Multi-Mode Microplate Reader from BioTek Instruments.

The production of iodine (I_2) by compounds in the presence of KI was assessed by irradiating, with white light (380–700 nm; LED system–25 mW.cm⁻²) for 120 min, a solution of each PS at 5.0 μM in presence of KI at 100 mM. The absorbance of I_2 at 340 nm was registered at pre-defined times.

General procedure

Prepare a 1M KI solution and dilute it 1:10 with PBS. Dilute all the compounds that you are going to test and make a 5μM solution for each one of them. Prepare the microwell plate by filling column A1 to C1 with PBS (250μL), then filling E1 to G1 with PBS+KI (25μL KI+ 225 PBS), and finally by filling Ax to Cx with the compound diluted in PBS (25μL compound+225μLPBS) and Ex to Gx with compounds diluted with PBS+KI (25μL compound + 25μL KI+ 200μL PBS). Go to the UV spectrometer and let it shake the plate for 15 minutes. When the shaking it's done take the first measurement (t_0). Put the plate under red light (25 mW/cm²) for 5 minutes. Shake the plate for just 30 seconds and then take another UV measurement. After you reach t_{15} (fourth measurement) put the plate under the red light for 15 minutes, and after that shake the plate for 30 seconds and take the UV measurement. Continue like this until you reach t_{120} (eleventh measurement)

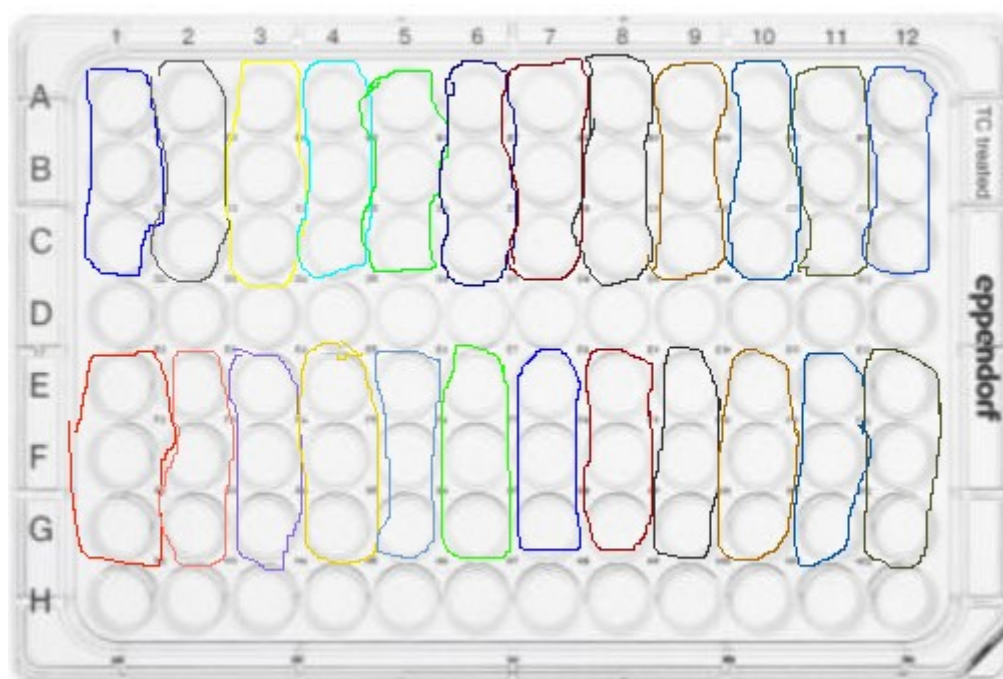


Figure 3.3.4a Compounds disposition: A1-C1 PBS, A2-C2 Mono DBU, A3-C3 DisubC DBU, A4-C4 Trisub DBU, A5-C5 Tetra DBU, A6-C6 Tetra DBN, A7-C7 Mono DBN, A8-C8 Disub T DBN, A9-C9 Disub C DBN, A10-C10 Disub T DBU, A11-C11 TPFPF, A12-C12 Trisub DBN; E1-G1 KI, E2-G2 Mono DBU+KI, E3-G3 DisubC DBU+KI, E4-G4 Trisub DBU+KI, E5-G5 Tetra DBU+KI, E6-G6 Tetra DBN+KI, E7-G7 Mono DBN+KI, E8-G8 Disub T DBN+KI, E9-G9 Disub C DBN+KI, E10-G10 Disub T DBU+KI, E11-G11 TPFPF+KI, E12-G12 Trisub DBN+KI

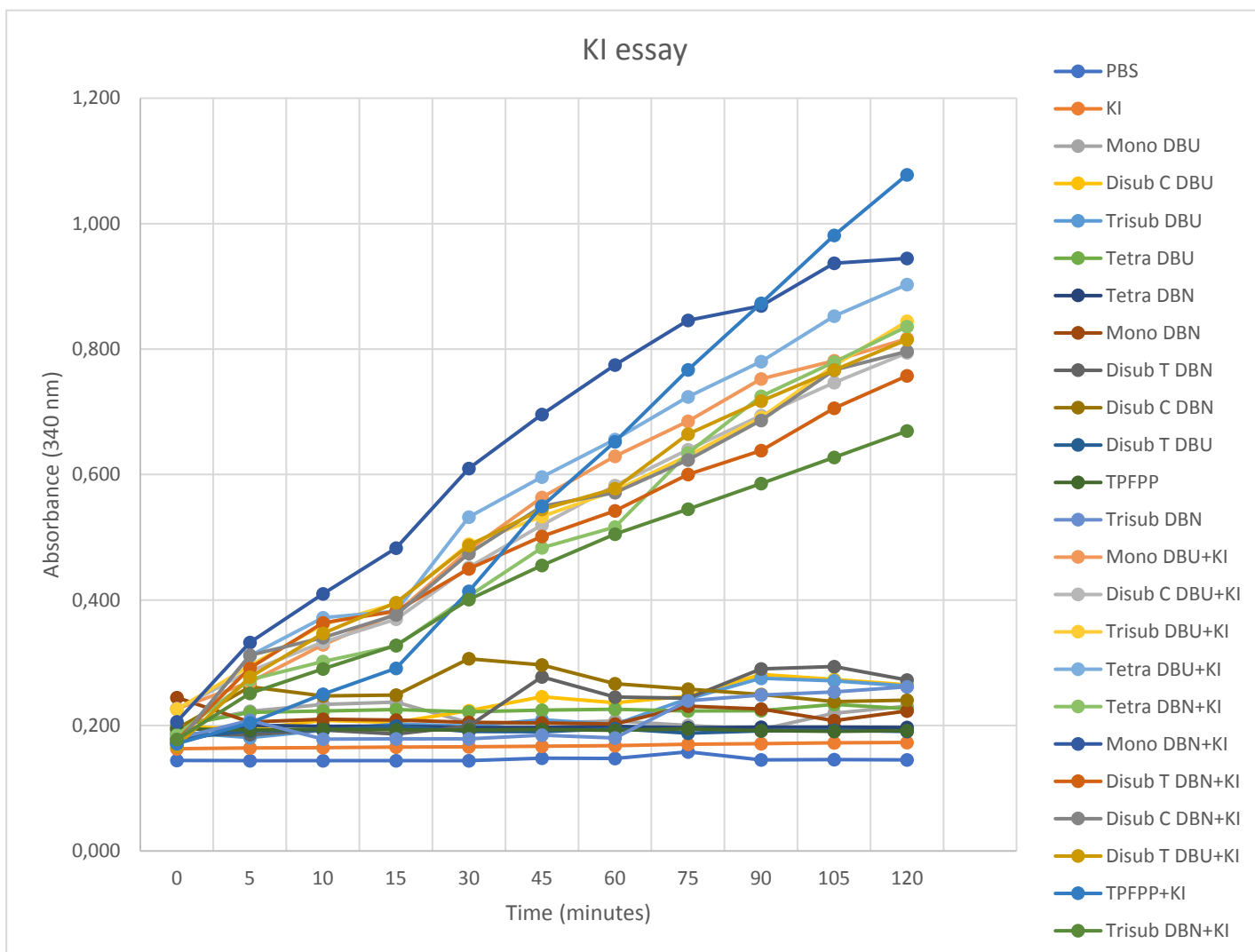


Figure 3.3.4b KI essay spectrum for TPFPP+DBU and TPFPP+DBN compounds

Chapter IV: Conclusions

4.1 Main Conclusions

Porphyrin synthesis is a time-consuming process, that gives low yields and require a lot of analysis. The solvent screening showed that acetonitrile was the best solvent to conduct all the synthesis, because it didn't interfere in the reaction, it's cheap, it's a class 2 ICH guidelines compound, easy to remove and gave the highest yields. The other solvents didn't make the cut because they didn't have some, or all of those features.

Finding the best temperature to work with, best reagent proportions and best extracting method was time consuming and with mixed results.

In the end the best way to synthesize the compounds was by slowly delivering the base in the reaction vial using a syringe pump. This increased the yield significantly and reduced the amount of "side products" produced.

DBU requires at least 1hr of reaction time to produce all the desired products, and the Yields are inconsistent even after repeating the same process several times in the same way.

DBN was a much better base to work with as it reacted faster and with better and consistent yields than DBU.

I never managed to get high yields for Compounds **2,3** and **7,8**, probably because the trisubstituted compound was more stable than the disubstituted one.

Compared to TPFPP, UV analysis showed that compounds **1,2,3** and **6,7,8** shifted slightly to the blue while compounds **4,5** and **9,10** shifted slightly to the red. The ϵ of all compounds were more or less comparable.

Fluorimetry analysis showed that the quantum yield of all compounds was lower than the TPP one. All those compounds won't be good tracers, as their quantum yield is too low.

Singlet oxygen generation test showed that all the compounds could generate the radical.

Compounds **5** and **10** though were the only one with singlet oxygen quantum yield high enough to be potentially effective (comparable to TPP), with compounds **4** and **9** not far behind.

KI singlet oxygen generation test showed that almost all compounds have the potential to be good photosensitizer if they are combined with KI, in particular compound **6**, **4**, and **TPFPP**.

Compounds **2,3** and **7,8** were among the worst one to generate singlet oxygen with both methods. Combining these results with the low yields, it makes them the less suitable for a potential PDT application.

Compounds **1** and **6** were the worst singlet oxygen generators with DMF, but **6** was one of the best with KI and **1** had better results with KI than with DMS.

The project goals were achieved as all compounds synthesis was optimized as best as I could, and had been fully characterized by UV spectroscopy, fluorescence emission, mass spectrometry, ^1H NMR, ^{12}C NMR, ^{19}F NMR, COSY, HMBC, HSQC, NOESY and singlet oxygen generation test.

Further in vitro biological studies for compounds **1,3,4,5,6,7,8,9,10** will be carried out using various tumor cells lines to test their potential application in phototherapy.

Side notes

Water as solvent using OHMIC showed that it's not viable as no products were synthesized.

However, adding NMP, or using only NMP as solvent produced some products.

OHMIC can be a suitable heating method to porphyrins with low solubility, but it will require more studies.

Chapter V: references

1. Milgrom, L. R.; *The Colours of Life: an Introduction to the Chemistry of Porphyrins and Related Compounds*. Oxford University Press: Oxford, 1997.
2. Quintas, A.; Freire, A. P.; Halpern, M. J., *Bioquímica - Organização Molecular da Vida*. Lidel: Lisboa, 2008.
3. N. Tsolekile, S. Nelana, and O. S. Oluwafemi, "Porphyrin as diagnostic and therapeutic agent," *Molecules*. 2019.
4. Wijesekera, T.; Dolphin, D., *Metalloporphyrins in Catalytic Oxidations – Synthetic Aspects of Porphyrin and Metalloporphyrin Chemistry*. Ed. Sheldon, R.A; Marcel Dekker Inc.: New York, 1994; Vol. 1, p. 193-239.
5. Kim, H. J.; Khalimonchuk, O.; Smith, P. M.; Winge, D. R., Structure, function and assembly of heme centres in mitochondrial respiratory complexes, *Biochim Biophys Acta*, 2012, 1823 (9), p. 1604-1616.
6. Smith, A.; Witty, M., *Heme, Chlorophyll, and Bilins: Methods and Protocols*. Ed. Smith, A.; Witty, M.; Humana Press, 2001.
7. A. T. P. C. Gomes, M. G. P. M. S. Neves, and J. A. S. Cavaleiro, "Cancer, photodynamic therapy and porphyrin-type derivatives," *An. Acad. Bras. Cienc.*, vol. 90, pp. 993–1026, 2018.
8. Vicente, M. G., *The Porphyrin Handbook - Synthesis and Organic Chemistry*, Ed. Kadish, K. M.; Smith, K. M.; Guillard, R.; Academic Press: San Diego, 2000; Vol.1 p.150-179.
9. Smith, K. M., *Porphyrins and Metalloporphyrins - General features of the structure and chemistry of porphyrin compounds*. Ed. Smith, K.M.; Elsevier: Amsterdam, 1975; p. 3-28.
10. G. P. Moss, "Nomenclature of tetrapyrroles. Recommendations 1986 IUPAC-IUB Joint Commission on Biochemical Nomenclature (JCBN).," *Eur. J. Biochem.*, 1988.
11. Soret, J. L., *Analyse spectrale: Sur le spectre d'absorption du sang dans la partie violette et ultra-violette*. *Compt. Rend. Acad. Sci.*, 1883; vol. 97, p. 1269- 1273.

12. N. Bhupathiraju, W. Rizvi, J. D. Batteas, and C. M. Drain, "Fluorinated porphyrinoids as efficient platforms for new photonic materials, sensors, and therapeutics.," *Org. Biomol. Chem.*, vol. 14 (2), pp. 389–408, 2016.
13. R. Giovannetti, "The Use of Spectrophotometry UV-Vis for the Study of Porphyrins," in *Macro To Nano Spectroscopy*, 2012, pp. 87–108.
14. Golubchikov, O.; Ageeva, T.; Symposium on Applications of Porphyrins in Medicine and the Fourth School for Young Scientists on the Chemistry of 87 Porphyrins and Related Compounds Ivanovo 2000. *Molecules*, 2000, 5 (12), p. 1461-1462.
15. M. Gouterman, "Optical Spectra and Electronic Structure of Porphyrins and Related Rings," in *The Porphyrins*, 1978.
16. Alea, M. E.; Duran, S.; Gonzalez, A.; Plaza, J. A.; Pérez- Garcia, L., Zinc metalloporphyrins-functionalised nano and microparticles as potential agents for photodynamic therapy, *Photodiagnosis and Photodynamic Therapy*, 2017, Vol. 17, p. A53
17. Janson, T. R.; Katz, J. J. *In The Porphyrins: Physical Chemistry- Part. B.* Dolphin, D. (Ed.); Academic Press: New York, 1978.
18. Rothmund, P., Formation of porphyrins from pyrrole and aldehydes. *J. Am. Chem. Soc.*, 1935, 57 (8), p. 2010-2011.
19. Rothmund, P., A New Porphyrin Synthesis. The Synthesis of Porphin, *J. Am. Chem. Soc.*, 1936, 58 (4), p. 625-627.
20. Rothmund, P.; Menotti, A. R., Porphyrin Studies. IV.1 The Synthesis of $\alpha,\beta,\gamma,\delta$ -Tetraphenylporphine, *J. Am. Chem. Soc.*, 1941, 63 (1), p. 267-270.
21. Lindsey, J. S., *The Porphyrin Handbook - Synthesis and Organic Chemistry*. Ed Kadish, K. M.; Smith, K. M.; Guillard, R.; Academic Press: New York, 2000; Vol. 1, p 45-112.
22. Adler, A. D.; Longo, F. R.; Finarelli, J. D.; Goldmacher, J.; Assour, J.; Korsakoff, L., A simplified synthesis for meso-tetraphenylporphine. *J. Org. Chem.* 1967, 32(2), p. 476.
23. Y. Zhu and R. B. Silverman, "Electronic effects of peripheral substituents at porphyrin meso positions," *J. Org. Chem.*, vol. 72, pp. 233–239, 2007.
24. J. J. Scheer, H.; Kats, "Porphyrins and Metalloporphyrins – Nuclear magnetic resonance spectroscopy of porphyrins and metalloporphyrins," 76 in *Porphyrins and Metalloporphyrins*, K. M. . Ed. Smith, Ed. Amsterdam: Elsevier Scientific Publishing Company:, 1975, pp. 399–524.

25. D. Shemin, "An illustration of the use of isotopes: the biosynthesis of porphyrins.," *Bioessays*, vol. 10, no. 1, pp. 30–35, 1989.
26. Lindsey, J. S.; Schreiman, I. C.; Hsu, H. C.; Kearney P. C. and Marquerattaz A. M.; (1987) Rothmund and Adler-Longo reactions revisited: synthesis of tetraphenylporphyrins under equilibrium conditions, *J. Org. Chem.*, 1967, Vol. 52, p. 827-836.
27. Goncalves, A. M. d'A.R.; Varejão, J. M. T. B.; Pereira, M. M., Some new aspects related to the synthesis of meso-substituted porphyrins. *J. Heterocycl. Chem.* 1991, 28 (2), p. 635-640.
28. Nascimento, B. F. O.; Pineiro, M.; Rocha Gonsalves, A. M. d'A.; Silva, M. R.; Beja, A. M.; Paixão, J. A., Microwave-assisted synthesis of porphyrins and metalloporphyrins: a rapid and efficient synthetic method, *J. Porphyrin Phthalocyanines*, 2007, 11 (2), p. 77-84.
29. Cavaleiro, J. A. S.; Tomé, A. C.; Neves, M. G. P. M. S. *In Handbook of Porphyrin Science; Vol.2;* Kadish, K.; Smith, K. M.; Guillard, R., Eds.; World Scientific Publishing Company: Singapore, 2010; p. 193-284.
30. Bonnett R., *Chemical Aspects of Photodynamic Therapy*, Gordon and Breach Science Publishers: London, 2000.
31. Wiehe, A.; Shaker, Y. M.; C. Brandt, J. C.; Mebs, S.; Senge, M. O., Lead structures for applications in photodynamic therapy. Part 1: Synthesis and variation of *m*-THPC (Temoporfin) related amphiphilic A2BC-type porphyrins, *Tetrahedron*, 2005, Vol. 61 (22), p. 5535-5564.
32. Hamblin, M. R.; Mróz, P., *Advances in Photodynamic Therapy: Basic, Translational, and Clinical – History of PDT: The first Hundred Years*, Ed. Hamblin, M.R.; Mroz, P.; Artech House Publishers, 2008.
33. Finsen N. R.; *Phototherapy*, Edwar Arnold Press: London, 1901.
34. T. Xu, R. Lu, X. Liu, P. Chen, X. Qiu, and Y. Zhao, "Porphyrins with four monodisperse oligocarbazole arms: Facile synthesis and photophysical properties," *J. Org. Chem.*, vol. 73(4), pp. 1809–1817, 2008.
35. Abdel-Kader, M. H., The Journey of PDT Throughout History: PDT from Pharos to Present in *Photodynamic Medicine: From Bench to Clinic*, Ed. Kostron, H.; Hasan, T., European society for Photobiology, 2016, p. 3-18.
36. Auler, H.; Banzer, G., *Untersuchungen über die rolle der porphyrine bei geschwulstkranken menschen und tieren. Z Krebsforsch*, 1942, Vol. 53, p. 65-68.
37. Figge, F. H. J.; Weiland, G. S.; Manganiello, L.O.J. Cancer detection and therapy. Affinity of neoplastic, embryonic, and traumatized tissues for porphyrins and metalloporphyrins. *Proc. Soc. Exp. Biol. Med.*, 1948, Vol. 68 (2), p. 640-641.
38. Pandey, R. K.; Zheng, G., *The Porphyrin Handbook - Applications: Past, Present and Future*. Ed. Kadish, K. M.; Smith K. M.; Guillard, R.; Academic Press: New York, 2000; Vol. 6, p. 157-230.

39. S. M. A. Pinto, C. S. Vinagreiro, V. A. Tomé, G. Piccirillo, L. Damas, and M. M. Pereira, "Nitrobenzene method: A keystone in meso -substituted halogenated porphyrin synthesis and applications," *J. Porphyr. Phthalocyanines*, vol. 23, pp. 329–346, 2019.
40. C. M. Che and J. S. Huang, "Metalloporphyrin-based oxidation systems: from biomimetic reactions to application in organic synthesis," *Chem. Commun.*, vol. 27, pp. 3996–4015, 2009.
41. J. I. T. Costa, A. C. Tomé, M. G. P. M. S. Neves, and J. A. S. Cavaleiro, "5,10,15,20-tetrakis(pentafluorophenyl)porphyrin: A versatile platform to novel porphyrinic materials," *J. Porphyr. Phthalocyanines*, vol. 15, pp.
42. Moan, J.; Peng Q.; *Photodynamic Therapy- An outline of the history of PDT*. Ed. Thierry Patric, 2003, p. 1-18.
43. Sternberg, E. D.; Dolphin, D.; Bruckner, C., Porphyrin-based Photosensitizers for use in Photodynamic Therapy. *Tetrahedron*, 1998, Vol. 54 (16), p. 4151-4202.
44. Dougherty, T. J., A brief history of clinical photodynamic therapy development at Roswell Park Cancer Institute. *J. Clin. Laser Med. Surg.*, 1996, Vol. 14, p. 219-221.
45. Hueger, B. E.; Lawter, J. R.; Waringrekar, V. H.; Cucolo, M. C., *Stable Freeze Dried Polyhematoporphyrin Ether/Ester*, United States Patent No. 5059619, 1991
46. Muller P. J.; Wilson, P.C., *Int. Adv. Surg. Oncol.*, 1995, Vol. 11, p. 346.
47. N. V. S. D. K. Bhupathiraju, W. Rizvi, J. D. Batteas, and C. M. Drain, "ChemInform Abstract: Fluorinated Porphyrinoids as Efficient Platforms for New Photonic Materials, Sensors, and Therapeutics," *ChemInform*, vol. 14, pp. 389–408, 2016.
48. A. Almeida, M. A. Faustino, and M. G. P. Neves, "Antimicrobial Photodynamic Therapy in the Control of COVID-19," *Antibiotics*, vol. 9 (5), p. 320, 2020.
49. J. M. Dabrowski, L. G. Arnaut, and J. M. Dąbrowski, "Photodynamic Therapy (PDT) of Cancer: From a Local to a Systemic Treatment," *Photochem. Photobiol. Sci. Photochem.*, vol. 14, pp. 1765–1780, 2015.
50. L. G. B. Rocha, "Development of a novel photosensitizer for photodynamic therapy of cancer," University of Coimbra, 2016.
51. D. van Straten, V. Mashayekhi, H. S. de Bruijn, S. Oliveira, and D. J. Robinson, "Oncologic photodynamic therapy: Basic principles, current clinical status and future directions," *Cancers (Basel)*, vol. 9(2), p. 19, 2017.
52. Wöhrle, D.; Hirth, A.; Bogdahn-Rai, T.; Schnurpfeil, G.; Shopova, M., Photodynamic therapy of cancer: Second and third generation of photosensitizers. *Russ. Chem. Bull.*, 1998, Vol. 47 (4), p. 807-816

53. 56 Sternberg, E. D.; Dolphin, D.; Bruckner, C., Porphyrin-based Photosensitizers for Use in Photodynamic Therapy. *Tetrahedron* 1998, Vol. 54 (16), p. 4151-4202.
54. 57 Sessler, J. L.; Hemmi, G.; Mody, T. D.; Murai, T.; Burrell, A.; Young, S. W., Texaphyrins: Synthesis and Applications. *Acc. Chem. Res.* 1994, Vol. 27 (2), p. 43-50.
55. 58 Wöhrle, D.; Shopova, M.; Mtiler, S.; Milev, A. D.; Mantareva, V. N.; Krastev, K., K., Liposome-delivered Zn(II)-2,3-naptocyanines as potential sensitizers for PDT: synthesis, photochemical, pharmacokinetic and phototerapeutic studies, *J. Photochem. Photobiol. B: Biol.*, 1993, Vol. 21 (2-3), p. 155-165.
56. Akhlynina, T. V.; Jans, D. A.; Rosenkranz, A. A.; Statsyk, N. N.; Balashova, I. Y.; Toth, G.; Pavo, I.; Rubin, A. B.; Sobolev A. S., Nuclear targeting of chlorin e6 enhances its photosensitizing activity, *J. Biol. Chem.*, 1997, 272, p. 20328-20331.
57. Brown, S. B.; Brown, E. A.; Walker, I., The present and future role of of photodynamic therapy in cancer treatment, *The Lancet Oncology*, 2004, Vol. 5, p. 497-508.
58. Choi, Y. M.; Adelzadeh, L., Wu, J. J., Photodynamic therapy for psoriasis, *J. Dermatolog. Treat.*, 2015, Vol. 26 (2), p. 202-207.
59. Tandon, Y. K.; Yang, M. F.; Baron, E. D., Role of photodynamic therapy in psoriasis: a brief review, *Photodermatol. Photoimmunol. Photomed.*, 2008, Vol. 24 (4), p. 222-230.
60. Schmidt-Erfurth, U.; Hasan, T., Mechanisms of Action of Photodynamic Therapy with Verteporfin for the Treatment of Age-Related Macular Degeneration, *Survey of Ophthalmology*, 2000, Vol. 45, Num. 3.
61. Litvack, F.; Grundfest, W. S., et al, Effect of hematoporphyrin derivative and photodynamic therapy on atherosclerotic rabbits, *The American Journal of Cardiology*, 1985, Vol. 56, p. 667-671.
62. Castano, A. P.; Demidova, T. N.; Hamblin, M. R., Mechanisms in photodynamic therapy: part one-photosensitizers, photochemistry and cellular localization, *Photodiagnosis and Photodynamic Therapy*, 2004, Vol. 1, p. 279-293.
63. Yoon, I.; Li, J. Z.; Shim, Y. K., Advance in Photosensitizers and Light Delivery for Photodynamic Therapy, *Clinical Endoscopy*, 2013, Vol. 46 (1), p. 7-23.
64. Alves, E.; Faustino, M. A. F., Neves, M. G. P. M. S.; Cunha, Â.; Nadais, H.; Almeida, A., Potential applications of porphyrins in photodynamic inactivation beyond the medical scope, *Journal of Photochemistry and Photobiology C: Photochemistry reviews*, 2015, Vol. 22, p. 34-57.
65. Costa, L.; Faustino, M. A. F.; Neves, M. G. P. M. S.; Cunha, Â.; Almeida, A., Photodynamic Inactivation of Mammalian Viruses and Bacteriophages. *Viruses*, 2012, Vol. 4 (6), p. 1034-1074.

66. Nyman, E. S.; Hynnenen P. H., Research advances in the use of tetrapyrrolic photosensitizers for photodynamic therapy, *Journal of Photochemistry and Photobiology B: Biology*, 2004, vol. 73, p. 1-28.
67. Gerweck, L. E.; Vijayappa, S.; Kozin, S., Tumor pH controls the in vivo efficacy of weak acid and base chemotherapeutics. *Mol. Cancer Ther*, 2006, 5 (4), p. 1275-1279.
68. Kongshaug, M.; Moan, J.; Brown, S. B., The distribution of porphyrins with different tumour localising ability among human plasma proteins. *Br. J. Cancer* 1989, Vol. 59 (2), p. 184-188
69. Tannock, I. F.; Rotin, D., Acid pH in Tumors and Its Potential for Therapeutic Exploitation. *Cancer Res.* 1989, Vol. 49 (14), p. 4373-4384.
70. Robertson, C. A.; Hawkins Evans, D.; Abrahamse, H., Photodynamic therapy (PDT): A short review on cellular mechanisms and cancer research applications for PDT, *Journal of Photochemistry and Photobiology B: Biology*, 2009, Vol. 96, p. 1-8.
71. Dougherty, T. J.; Gomer, C. J.; Henderson, B. W.; Jori, G.; Kessel, D.; Korbelik, M.; Moan, J.; Peng, Q., Photodynamic Therapy. *J. Natl. Cancer Inst.* 1998, Vol. 90 (12), p. 889-905.
72. Allison, R. R; Sibata, C. H., Oncologic photodynamic photosensitizers: a clinical review, *Photodiagnosis and Photodynamic Therapy*, 2010, Vol. 7, p. 61-75
73. C. S. Foote, "Definition of type I and type II photosensitized oxidation," *Photochem. Photobiol.*, vol. 54(4), pp. 659-659, 1991.
74. A. P. Castano, T. N. Demidova, and M. R. Hamblin, "Mechanisms in photodynamic therapy: Part one - Photosensitizers, photochemistry and cellular localization," *Photodiagnosis Photodyn. Ther.*, vol. 1(4), pp. 279- 293, 2004.
75. E. Buytaert, M. Dewaele, and P. Agostinis, "Molecular effectors of multiple cell death pathways initiated by photodynamic therapy," *Biochim. Biophys. Acta - Rev. Cancer*, vol. 1776(1), pp. 86-107, 2007.
76. P. Wang, S. Sun, H. Ma, S. Sun, D. Zhao, S. Wang, and X. Liang, "Treating tumors with minimally invasive therapy: A review," *Materials Science and Engineering C*. 2020.
77. C. S. Vinagreiro, N. P. F. Goncalves, M. J. F. Calvete, F. A. Schaberle, L. G. Arnaut, and M. M. Pereira, "Synthesis and characterization of biocompatible bimodal meso-sulfonamide-perfluorophenylporphyrins," *J. Fluor. Chem.*, vol. 180, pp. 161-167, 2015.
78. T. Goslinska and J. Piskorz, "Fluorinated porphyrinoids and their biomedical applications," *J. Photochem. Photobiol.*, pp. 304- 321, 2011.
79. D. E. Yerien, S. Bonesi, and A. Postigo, "Fluorination methods in drug discovery," *Org. Biomol. Chem.*, vol. 14, pp. 8398-8427, 2016.

80. M. Vangala and G. P. Shinde, "p-Nitrophenyl carbonate promoted ringopening reactions of DBU and DBN affording lactam carbamates," *Beilstein J. Org. Chem.*, 2016, doi: 10.3762/bjoc.12.197.
81. A. M. Hyde, R. Calabria, R. Arvary, X. Wang, and A. Klapars, "Investigating the Underappreciated Hydrolytic Instability of 1,8- Diazabicyclo[5.4.0]undec-7-ene and Related Unsaturated Nitrogenous Bases," *Org. Process Res. Dev.*, 2019, doi: 10.1021/acs.oprd.9b00187.
82. W. C. Shieh, S. Dell, and O. Repič, "Nucleophilic catalysis with 1,8- diazabicyclo[5.4.0]undec-7-ene (DBU) for the esterification of carboxylic acids with dimethyl carbonate," *J. Org. Chem.*, 2002, doi: 10.1021/jo011036s.
83. R. Nirmala, T. Ponpandian, B. R. Venkatraman, and S. Rajagopal, "Nucleophilic behaviour of DBU towards imidazolides: One-pot synthesis of ϵ -caprolactam derived carbamates and amides," *Tetrahedron Lett.*, 2013, doi: 10.1016/j.tetlet.2013.07.056.
84. F. Tessari, "Novel porphyrin-based conjugates: synthesis and photophysical characterization," *Università degli studi di Padova - Universidade de Aveiro*, 2018.
85. 9 August 2019 EMA/CHMP/ICH/82260/2006 Committee for Human Medicinal Products ICH guideline Q3C (R6) on impurities: guideline for residual solvent
86. Ohmic Heating: An Emerging Concept in Organic Synthesis: Vera L. M. Silva,*[a] Luis M. N. B. F. Santos,[b] and Artur M. S. Silva*[a]
87. Cationic Pyrrolidine/Pyrroline-Substituted Porphyrins as Efficient Photosensitizers against *E. coli* Bruno M. F. Ladeira 1, Cristina J. Dias 1, Ana T. P. C. Gomes 2 , Augusto C. Tomé 1 , Maria G. P. M. S. Neves 1 , Nuno M. M. Moura 1,* , Adelaide Almeida 2,* and M. Amparo F. Faustino 1,*